People's Democratic Republic of Algeria
Ministry of Higher Education and Scientific Research
University of Adrar
Faculty of Science of Matter, Mathematics, and Computer Science

N° 12 - FSMMI/CSD-SM/2025

Certificate of Scientific Production

We hereby certify, Chairman of the Scientific Committee of the Department of Matter Sciences of the Faculty of Mathematical and Computer Sciences, that the teacher :

Dr.SAKHER Elfahem,Associate Professor, Class "A"Has produced a course handout entitled **Nanotechnology**for the 2024/2025 academic year. This handout conforms to the taught program and is intended forthe 1st Master: Energy Physics and Renewable Energies.

The pedagogical document has undergone expert review under the auspices of the Departmental Scientific Council (DSC) and has received a favourable opinion for its editing and publication in the university library and on the website of the University of Adrar.

Adrar, May 5, 2025

President of the DSC

د. سليماني سعيد
رئيس اللجنة العلمية لقسم علوم المادة

اللجنة العلمية
لقسم علوم المادة

Algerian Democratic and Popular Republic
Ministry of Higher Education and Scientific Research
AHMED DRAIA UNIVERSITY -ADRAR

Faculty of Material Sciences,
Mathematics and Computer
Science.
Department of Material
Sciences

COURSE HANDOUT.

NANOTECHNOLOGY

Field: Material Sciences

Course: 1st Master: Energy Physics and Renewable Energies

Unit: Discovery Teaching (UED 1.1)

Subject: Nanotechnology

Total hourly volume: 22h30 hours (1 course)

Number of credits: 2

Prepared by:

Dr. Elfahem SAKHER

Lecturer "A"

2024-2025

Foreword

Nanotechnology is an exciting and constantly evolving field that encompasses the study, design, synthesis, and manipulation of materials, devices, and systems at the nanoscale (1 nm = 10^{-9} m). This course, designed for first-year Master's students in Energetic Physics and Renewable Energies, aims to provide an in-depth introduction to the fundamental concepts and practical applications of nanotechnologies as part of the Discovery Teaching Unit (UED 1.1).

The course curriculum is structured to provide an overview of the underlying principles of nanotechnology, as well as fabrication and characterization methods at the nanoscale. Students will also explore how nanotechnologies can be applied across various fields, including electronics, medicine, the environment, and renewable energy.

The total course duration is 22 hours and 30 minutes, distributed across several sessions of theoretical and practical lessons. At the end of the semester, students will be assessed on their knowledge and understanding of the concepts and techniques covered and will earn 2 credits upon successful completion of the course.

The specific objectives of the course include:

- Understanding the fundamental principles of nanoscience and nanotechnology.
- Familiarizing with synthesis and fabrication techniques for nanostructures and nanomaterials.
- Acquiring skills in characterization methods for materials at the nanoscale.
- Analyzing and evaluating the impact of nanotechnologies on society, the economy, and the environment.
- Exploring the applications of nanotechnologies in energy, health, the environment, and electronics.

Table of Contents

I. Introduction :

The concept of nanotechnology, which involves the manipulation and control of matter on an atomic and molecular scale, was first introduced during a landmark lecture in 1959 by the physicist Richard Feynman titled *"There's Plenty of Room at the Bottom."* During this visionary talk, Feynman outlined the immense possibilities of working at the nanoscale, where individual atoms and molecules could be observed, arranged, and utilized. At the time, the practical realization of his ideas seemed far off, but his insights laid the foundational thinking for a revolutionary field. Decades later, Feynman's vision has not only been realized but has also transformed into a thriving area of research and innovation, fundamentally changing numerous industries and aspects of modern society.

Nanotechnology has emerged as one of the most dynamic and rapidly expanding interdisciplinary sciences. It bridges traditionally distinct disciplines, including engineering, biology, chemistry, physics, and medicine, fostering a collaborative approach to solving complex problems. By enabling scientists to manipulate matter at a scale of 1 to 100 nanometers, nanotechnology unlocks the ability to design materials and devices with unprecedented precision and functionality. Structures at this scale exhibit unique physical, chemical, and optical properties, which are often markedly different from their bulk counterparts.

One of the most compelling aspects of nanotechnology is its ability to observe and manipulate individual atoms and molecules, as depicted in Figure 1. This capability has led to the development of specialized fields like nano-optics, which focuses on the behavior of light and its interactions with nanostructures.

The nanoscale size range of 1 to 100 nanometers not only provides a platform for cutting-edge research but also opens doors to groundbreaking applications across sectors such as healthcare, energy, electronics, and environmental science.

In essence, nanotechnology represents a profound shift in how we approach material science, offering tools to engineer solutions at the atomic level with precision that was once unimaginable. This convergence of disciplines and techniques heralds a new age of scientific exploration and technological innovation, continuing to expand the boundaries of what is possible.

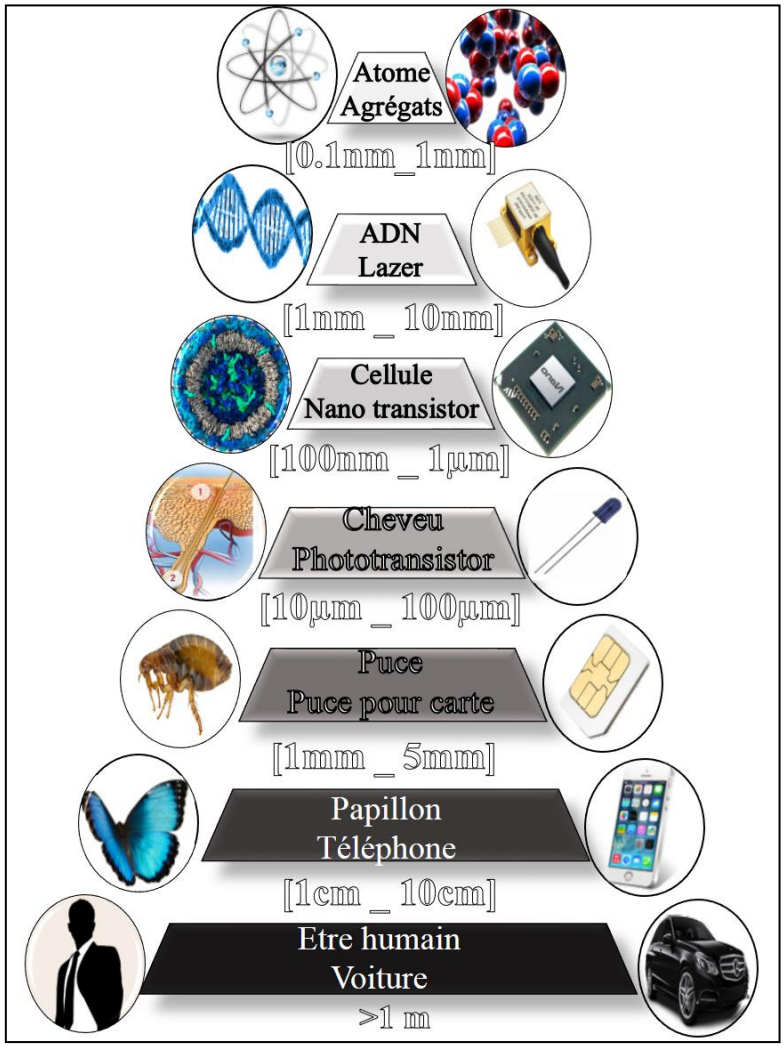

Figure 1: Visual Examples of the Size and Scale of Nanotechnologies.

By leveraging the unique phenomena that naturally occur at the nanoscale, scientists have unlocked the ability to transform everyday materials, enabling them to exhibit properties previously deemed unimaginable. At this scale, characteristics such as melting point, color, electrical conductivity, magnetic permeability, and chemical

reactivity become highly dependent on particle size. This profound shift in behavior arises from the fundamental differences between materials in their bulk form and their nanometric counterparts.

When engineered at nanometric dimensions, materials undergo significant alterations in their intrinsic properties. For instance, gold—a material known for its distinct golden hue—appears red or violet at the nanoscale due to changes in how its surface electrons interact with light. Such transformations highlight the novel behaviors materials can exhibit when reduced to nanoscale dimensions.

One of the defining characteristics of nanomaterials is their substantially increased relative surface area. As the size of a particle decreases, the surface area-to-volume ratio rises dramatically. This means a higher proportion of the atoms are located on the surface rather than within the particle's interior. For example, while a particle measuring 30 nm may have approximately 5% of its atoms on the surface, a 3 nm particle can have as much as 50%. As a result, a given mass of nanoparticles provides a far greater number of surface atoms than the same mass of larger particles. This enhanced surface exposure significantly increases the material's interaction with its surroundings, leading to heightened chemical reactivity, improved catalytic efficiency, and altered mechanical and electrical properties.

The increased surface area, however, is not the only factor contributing to the unique behavior of nanomaterials. At these scales, quantum effects—phenomena that arise from the confinement of electrons within the tiny dimensions of nanostructures—begin to dominate. These effects become particularly pronounced when the particle size is reduced to just a few tens of nanometers, altering the material's optical, electrical, and magnetic properties in ways not observed in bulk materials. For instance, quantum confinement can shift the energy levels of electrons, thereby changing a material's color or electrical behavior.

Taken together, the combination of increased surface area and quantum effects provides nanomaterials with remarkable properties that can be precisely tailored for advanced applications. These unique attributes underpin the transformative potential of nanotechnology, enabling innovations in fields ranging from energy storage and environmental remediation to medicine and electronics.

II. Nanomaterials:

II.1 Nanostructured Materials:

Nanostructured materials are generally defined as materials composed of polycrystals that can be either single-phase or multi-phase. These materials contain a significant proportion of atoms located at the grain boundaries, a feature that can endow them with interesting properties not found in their bulk counterparts.

The structure of nanomaterials can be seen as comprising two parts: a crystalline core (with structure, lattice parameter, etc.) and an outer portion formed by the interface (a zone with vacancies, defects, and possibly impurities).

Nanocrystalline materials exhibit superior properties compared to materials with larger grain sizes, due to the enhanced presence of interfaces and a large surface area-to-volume ratio. Among these enhanced properties are: increased hardness, amplified diffusivity, improved ductility, reduced density, decreased elastic modulus, increased electrical resistivity, higher specific heat, greater thermal expansion coefficient, lower thermal conductivity, and improved soft magnetic properties.

Their applications are incredibly diverse, ranging from creating more selective anti-pollution filters, to more reliable electronic components, to stronger plastics, and beyond.

II.2 Classification of Nanomaterials:

Nanomaterials can be systematically categorized into four main families based on their dimensional characteristics and modes of utilization. Each family encompasses materials with unique forms and functionalities (see Figure .2).

a) Zero-Dimensional Nanomaterials

Zero-dimensional nanomaterials are composed of clusters of atoms that may be randomly dispersed or organized into defined structures. These materials are isotropic

in nature, meaning they exhibit the same properties in all directions due to their lack of extended dimensions.

b) One-Dimensional Nanomaterials

These materials have one extended dimension and include structures such as nanowires and nanotubes:

- **Nanowires:**

Monocrystalline structures with diameters typically in the range of tens of nanometers.

Their lengths can vary widely, from approximately 500 nm to several micrometers (up to 10 µm).

They exhibit exceptional electrical, optical, and mechanical properties, making them ideal for nanoscale devices.

- **Nanotubes:**

Tubular structures with diameters as small as 1–2 nm and lengths extending up to 1 mm.

Carbon nanotubes (CNTs) are the most well-known, prized for their extraordinary strength, electrical conductivity, and thermal stability.

c) Two-Dimensional Nanomaterials

These materials are defined by their lamellar structures or thin layers. Examples include:

- **Deposited Clusters:** Thin films created via plasma spraying, chemical vapor deposition (CVD), or electrochemical methods.
- **Coatings:** Thick coatings that provide enhanced surface properties like wear resistance, corrosion protection, or improved optical characteristics.

d) Three-Dimensional Nanomaterials

Three-dimensional nanomaterials are compact structures that exhibit nanoscale features throughout their bulk. Examples include:

- **Nanoceramics:** Materials with enhanced hardness and thermal stability, used in high-performance applications such as cutting tools and biomedical implants.
- **Nanostructures:** Complex assemblies of nanocrystals forming interconnected networks.

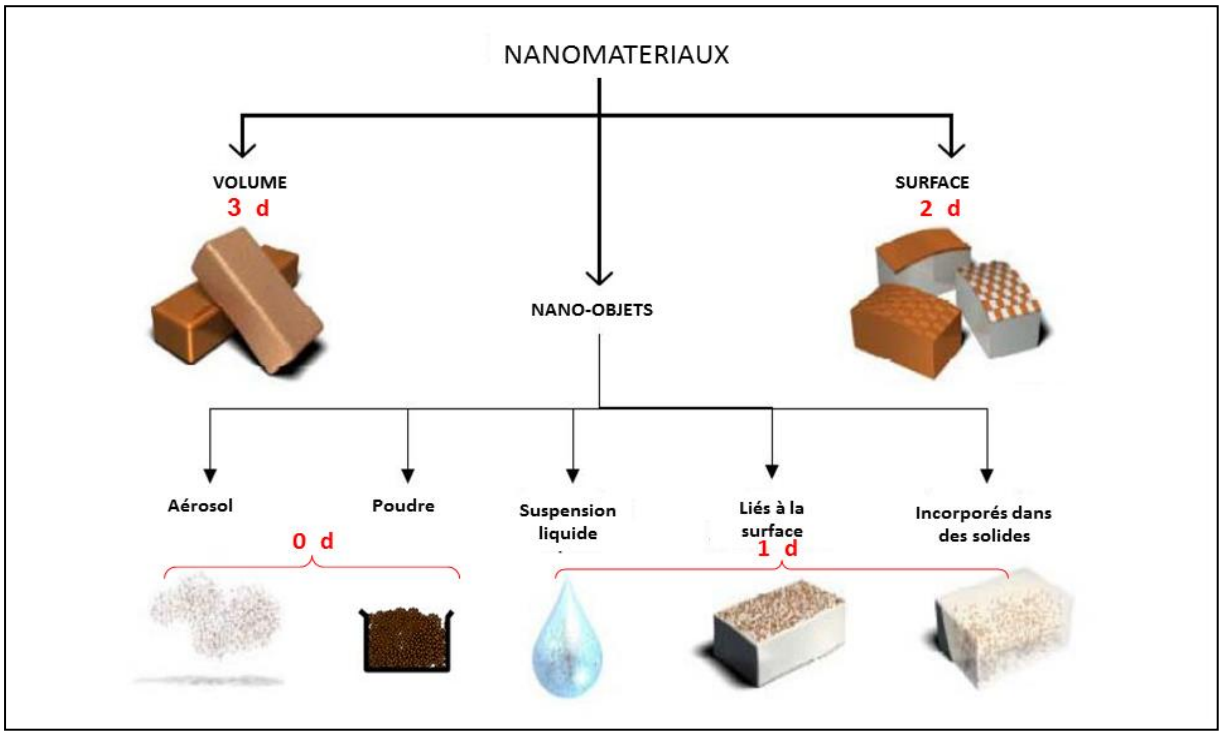

Figure 2 : Representation of Types of Nanostructured Materials

II.3 Properties of Nanomaterials:

The advancement of techniques for fabricating materials at nanometric dimensions has unlocked a broad and dynamic field of exploration, revealing novel properties across various physical domains such as optics, electronics, and magnetism. These nanoscale properties have already found applications in diverse industries, ranging from catalysis to mechanical engineering. However, the widespread application of

nanomaterials, particularly in structural materials, faces challenges due to the difficulty in producing them in large quantities and the high associated costs.

In parallel with these developments, emerging technologies have enabled the precise shaping and modification of material systems at the nanometric scale, either by adjusting their composition or through advanced machining techniques. These innovations have laid the groundwork for the creation of groundbreaking devices that are critical to the future of fields such as microelectronics and computing. While the potential applications of such advancements are vast, a detailed exploration of their full scope lies beyond the limits of this discussion.

II.3.1 Physical Properties

The nanoscale dimensions of materials bring about significant changes in their physical properties, primarily due to the emergence of quantum phenomena. These phenomena, which have been studied in physics for nearly a century, endow nanomaterials with characteristics that are strikingly different from those of their bulk counterparts.

One of the defining features of nanomaterials is their extraordinarily high surface-to-volume ratio, which has profound implications for their structural and functional properties. As particle size decreases, the proportion of atoms located at the surface increases significantly. This emphasis on surface and interface effects leads to altered properties, including enhanced reactivity, mechanical behavior, and optical characteristics. These surface-dominated effects have been the focus of a growing body of research, underscoring their importance in the study of nanomaterials.

a) Quantum Confinement and Its Effects

At the nanometric scale, the spatial confinement of electrons alters the electronic properties of materials, introducing quantum effects. This electronic confinement arises when the dimensions of the material become comparable to the de Broglie wavelength of electrons. As a result:

b) **Quantum Wells (QWs):** Two-dimensional nanostructures with nanometric thicknesses that restrict electronic motion to two dimensions. This confinement changes the way charge carriers move and interact, leading to entirely new transport properties.

c) **Dimensional Reduction:** In nanostructures, electronic transport transitions from three-dimensional (3D) behavior in bulk materials to two-dimensional (2D) or even one-dimensional (1D) behavior in structures like nanowires or nanotubes. This shift has profound implications for electronic and optoelectronic devices.

These quantum effects not only alter electronic properties but also influence optical, magnetic, and thermal characteristics, making nanomaterials highly versatile and valuable for advanced applications.

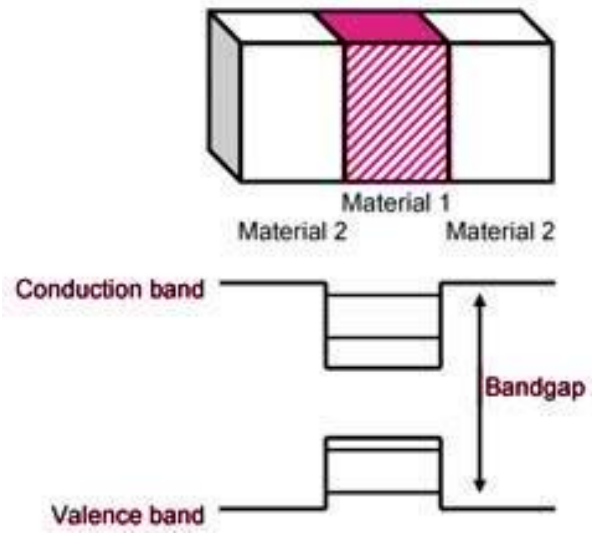

Figure 3 : Two-dimensional nanostructures (quantum wells)

The development of new deposition techniques has been instrumental in harnessing the unique properties of nanomaterials. For instance:

The creation of two-dimensional structures like quantum wells allows researchers to explore and manipulate electronic transport properties.

These techniques have enabled precise control over material dimensions and composition, facilitating the design of nanomaterials with tailored functionalities.

However, it is essential to acknowledge the variability in experimental findings. Early studies on nanocrystalline materials often relied on gas-condensation techniques, which require consolidation steps. Many of these results have since been found to conflict with data obtained from more recent synthesis methods that avoid such steps. Modern techniques, such as atomic layer deposition (ALD) and chemical vapor deposition (CVD), offer greater precision and reproducibility, contributing to a deeper understanding of nanoscale phenomena.

II.3.2 Energy and Diffusion:

The thermodynamic and kinetic behavior of nanomaterials is predominantly influenced by grain boundaries. At the nanoscale, surface energies become comparable to volume energies, necessitating the inclusion of surface tension in the free enthalpy expression:

$$G^* = G - 4\gamma_s \frac{V}{L} \qquad (1)$$

Here, V is the atomic volume; L is the grain size; γs is the surface energy of the grain, dependent on its environment. This energy is a function that increases as L decreases.. Consequently, material properties tied to energy—such as specific heat, elastic modulus, and thermal expansion coefficient—reflect the influence of reduced energy at the nanoscale.

In nanocrystals, the activation energy for diffusion is approximately three times lower than in their micrometer-scale counterparts. Enhanced grain boundary mobility facilitates grain growth at relatively low temperatures. However, the presence of impurities restricts this growth by exerting a pinning effect at grain boundaries, thereby lowering their energy and diminishing the thermodynamic driving force for grain enlargement.

This heightened diffusivity profoundly affects several mechanical and material properties. For instance, nanomaterials exhibit increased superplasticity, efficient

doping at reduced temperatures, and the capability to synthesize materials containing immiscible elements at significantly lower temperatures compared to coarse-grained materials. These effects are attributed to the higher solubility limit in the solid state. Additionally, the observed increase in diffusivity is often linked to the presence of porosity in consolidated samples, which further enhances mass transport.

II.3.3 Thermal Expansion:

Nanocrystalline materials exhibit a higher coefficient of thermal expansion compared to materials with micrometric grain sizes. This is primarily due to the substantial interfacial volume present in nanomaterials, which significantly influences their thermal behavior.

For example, nanocrystalline copper with a grain size of 8 nm, synthesized via inert gas condensation, has a measured thermal expansion coefficient of approximately $31x10^{-6}$ K^{-1}. This value is notably double that of monocrystalline copper, highlighting the pronounced effect of grain size on thermal properties.

In contrast, for electro-deposited nanocrystalline nickel, the thermal expansion coefficient closely matches that of polycrystalline nickel within the temperature range of 140–500 K. This similarity suggests that the influence of nanostructuring on thermal expansion may vary depending on the material and the processing method used.

II.3.4 Electrical Properties:

The integration of nanoparticles and nanotubes into materials significantly modifies their electrical conductivity, even in materials traditionally considered insulators. This effect is particularly pronounced when carbon nanotubes (CNTs) are used as fillers due to their exceptional electrical properties.

II.3.4.1 Role of Carbon Nanotubes

a) Percolation Threshold:

At low concentrations of CNTs, a conductive network can form within the material, enabling the transport of charge carriers.

This phenomenon, known as the percolation threshold, allows materials with minimal CNT content to transition from insulating to conductive behavior.

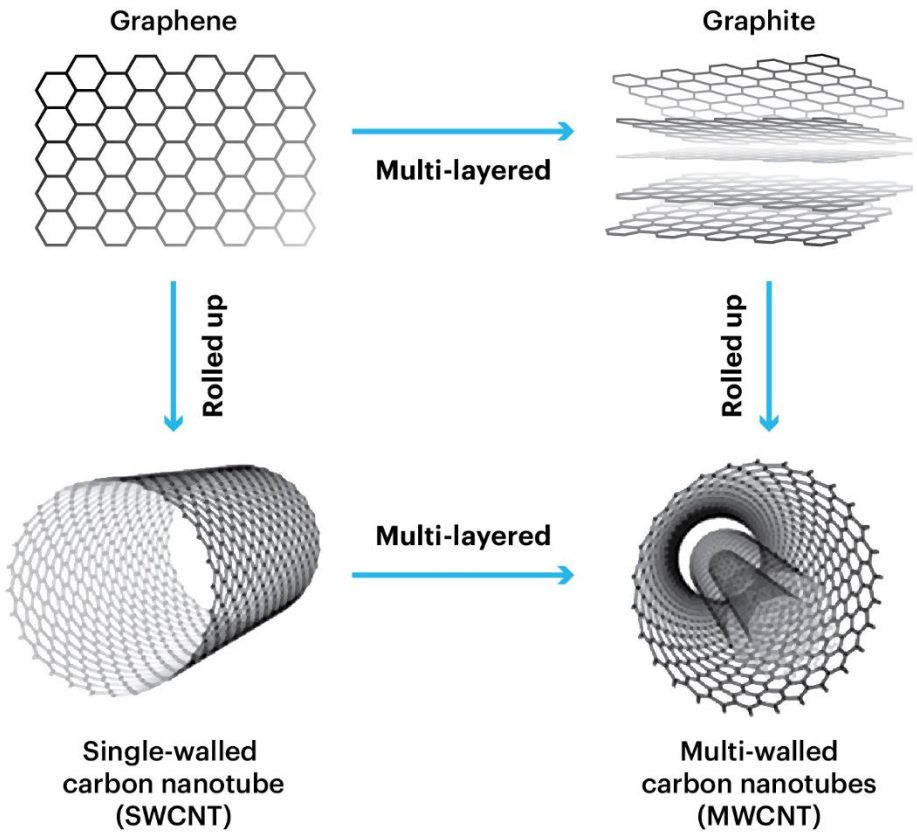

Figure 4: Carbon nanotubes (CNTs)

II.3.4.2 Mechanisms of Conductivity:

The high aspect ratio and quasi-metallic nature of CNTs facilitate the formation of continuous pathways for electron flow.

Conductivity arises through direct contact between nanotubes or electron tunneling across small gaps, enhancing charge carrier mobility.

II.3.5 Optical Properties:

Nanoparticles possess unique optical properties due to their dimensions, which are smaller than the wavelengths of visible light (380–780 nm). This nanoscale size enables significant alterations in light interaction, resulting in enhanced transparency, scattering, and absorption.

II.3.5.1 Transparency and Light Scattering

a) Reduced Scattering:

The small size of nanoparticles minimizes light scattering, leading to improved transparency in the host material.

This property is particularly evident in thin films and coatings.

b) Structural Influence:

The size, shape, and distribution of nanoparticles play a crucial role in determining the material's optical behavior, particularly in reducing opacity and enhancing clarity.

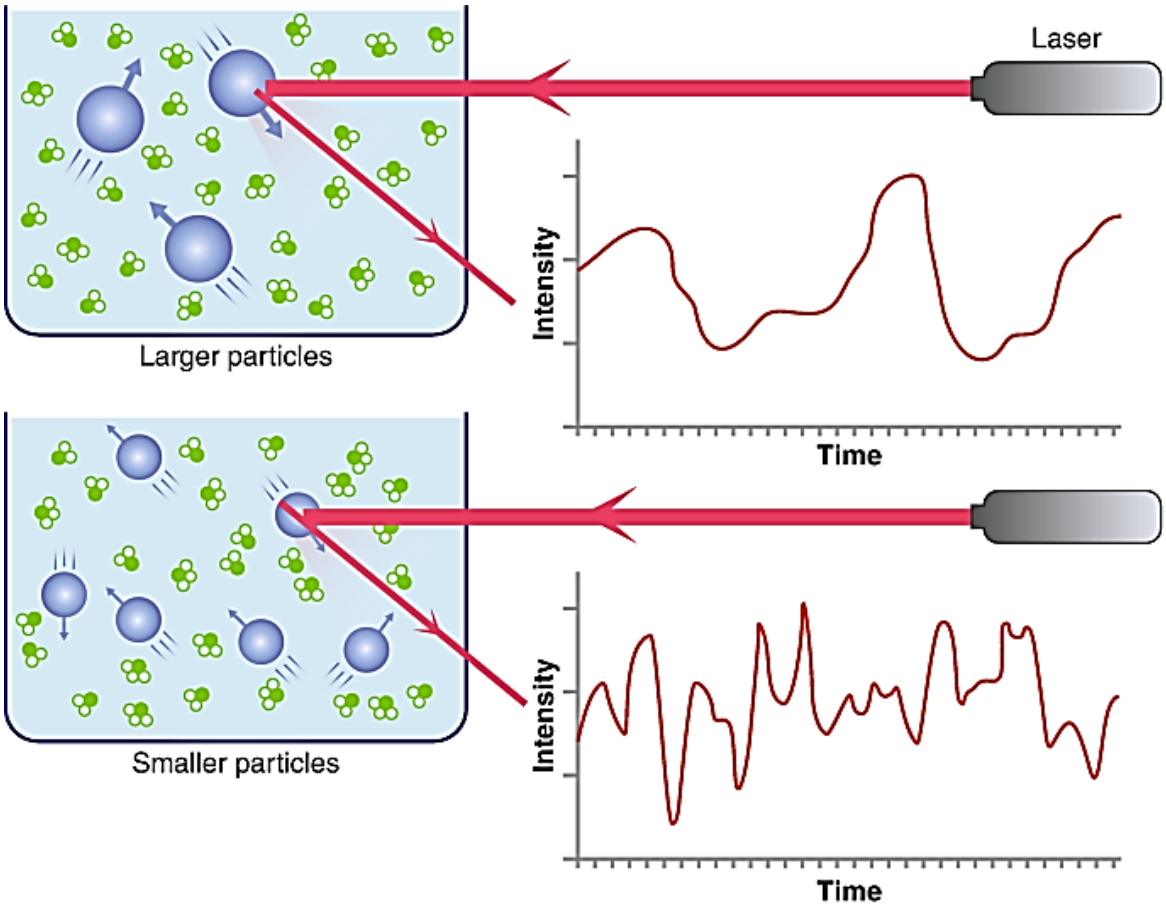

Figure5: Particule sise effect on Transparency and Light Scattering

II.3.6 Magnetic Properties:

The size of crystalline domains plays a pivotal role in determining the magnetic behavior of materials, often leading to significant technological advancements. Even materials traditionally classified as non-magnetic or antiferromagnetic can develop a magnetic moment when reduced to very small particle sizes.

For instance, in nanostructured alloys, a reduction in particle size is associated with enhanced coercive fields and remanent magnetization. This is primarily due to the increasing influence of the atomic fraction at the surface and/or interface, which becomes a dominant factor as particle size decreases. Key intrinsic magnetic properties such as saturation magnetization and magneto-crystalline anisotropy are profoundly affected by particle size.

In ferromagnetic materials, the disordered atomic arrangement and fewer atomic neighbors at the surface contribute to a reduction in saturation magnetization as particle size decreases. However, below a certain threshold, the surface anisotropy contribution can become significant, leading to an overall increase in the total anisotropy energy as particle size diminishes.

Figure 6 (a) illustrates the evolution of the coercive field with changing crystalline domain size. This progression reveals a transition from magnetically soft behavior to magnetically hard behavior and, eventually, to superparamagnetic characteristics. The advent of nanomaterials in the field of magnetism has enabled the creation of new materials with variable coercive and saturation fields, previously unattainable with conventional materials.

As shown in Figure 6 (b), for relatively large grain sizes, the coercive field is lower, as exemplified in permalloy. With decreasing grain size, the coercive field initially increases inversely with grain size (1/D), where (D) represents the grain size. Upon entering the nanocrystalline domain, the coercive field begins to decrease

proportionally to the sixth power of the grain size (D^{-6}), eventually transitioning into the amorphous domain. These changes underscore the intricate interplay between grain size and magnetic properties, offering opportunities for tailoring materials for specific magnetic applications.

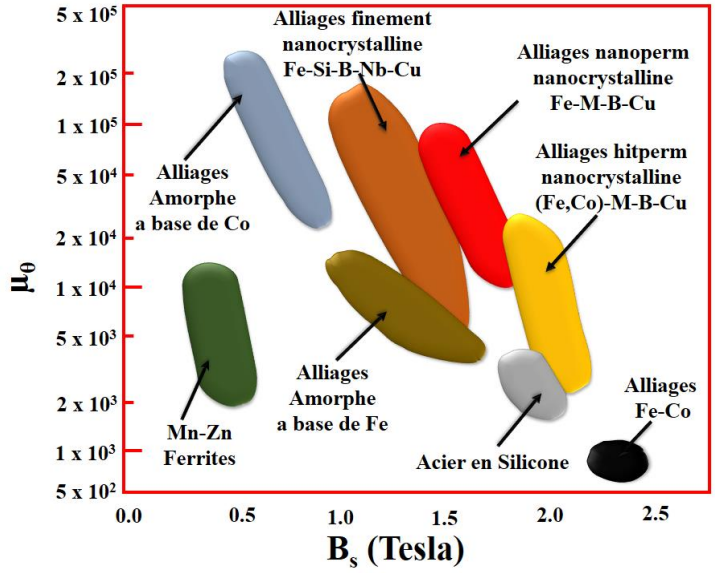

(a)

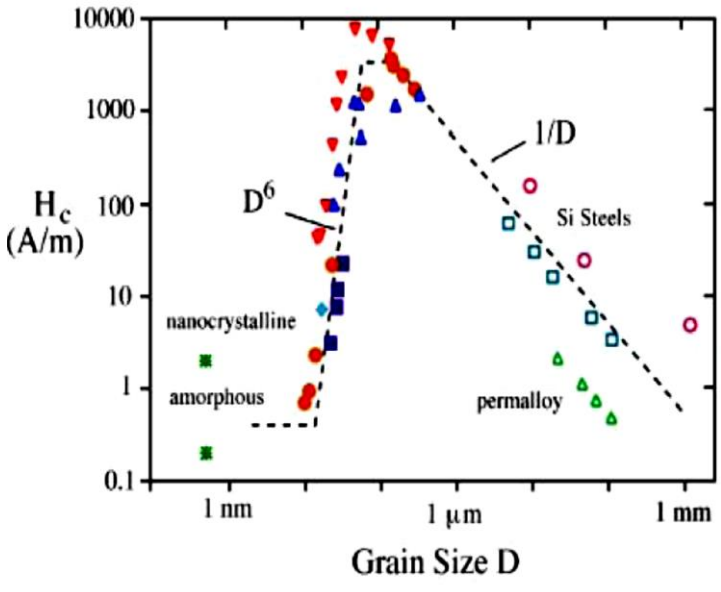

(b)

Figure 6*:* Modification of the Coercive Field as a Function of

(a) Size of the crystalline domains.

(b) Grain size for soft magnetic alloys.

II.3.6.1 Magnetic Domains and Domain Walls

Ferromagnetic materials exhibit spontaneous magnetization below their Curie temperature(Tc), yet they are typically observed in a demagnetized state with a net magnetization of zero. This apparent contradiction arises from the internal structure of the material and was first explained in 1907 by Weiss, who introduced the concept of magnetic domains.

Weiss proposed that ferromagnetic materials are divided into elementary volumes, known as Weiss domains, each of which possesses spontaneous magnetization. However, the magnetization direction varies between domains, resulting in a macroscopic state of zero net magnetization when no external magnetic field is present. This arrangement minimizes the material's demagnetizing energy, balancing the internal magnetic forces.

When an external magnetic field is applied, certain domains are energetically favored, and their influence grows as less favorable domains diminish. This process occurs through the movement of domain walls, which are the boundaries between adjacent magnetic domains.

These domain walls, also known as Bloch walls, serve as transition zones where the magnetic moments gradually rotate. Within a Bloch wall, the magnetic moments shift from alignment with the magnetization direction of one domain to that of the adjacent domain. The energy associated with the demagnetizing field due to wall formation is remarkably low, which underscores the efficiency of this structural arrangement in minimizing overall energy .

This interplay of magnetic domains and domain walls is fundamental to the understanding of ferromagnetic materials, influencing their behavior in both demagnetized and magnetized states. It also provides a framework for manipulating their magnetic properties for technological applications..

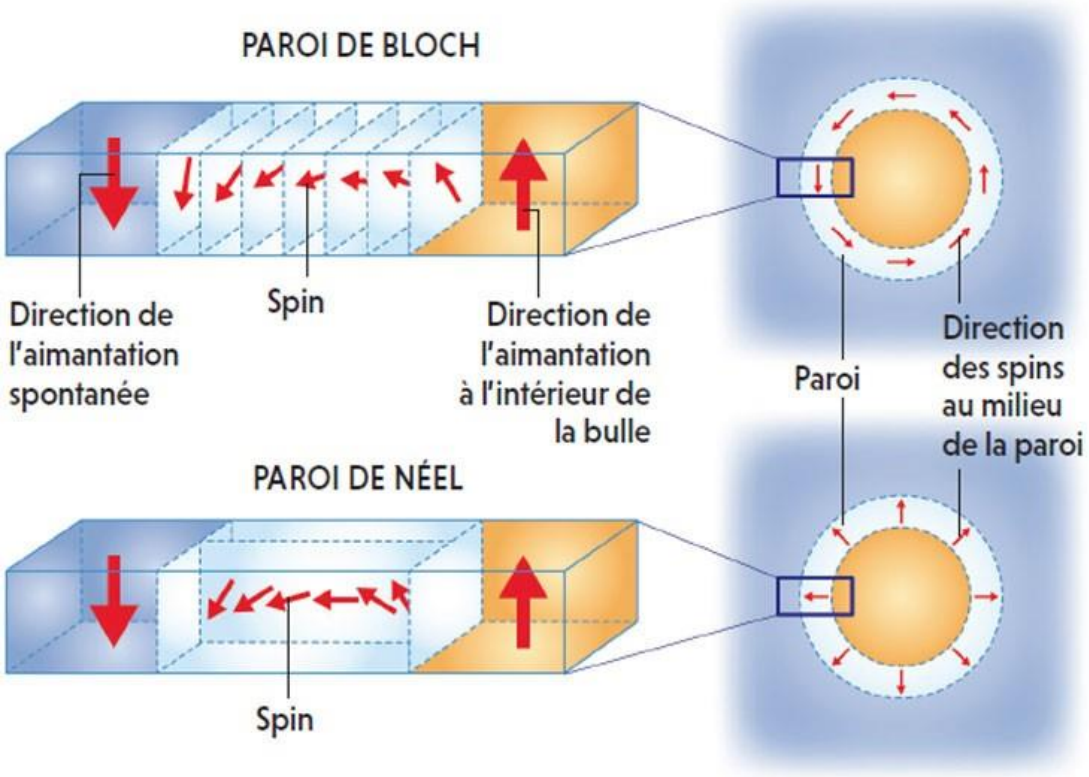

Figure 7: Structure of the Thin Transition Layer (or Wall) Between Domains

Within magnetic domain walls, the magnetic moments are neither completely parallel to one another nor aligned along an easy magnetization direction. This misalignment results in energy loss during wall formation, referred to as wall energy. The magnitude of this energy is governed solely by the interplay between two competing forces: the anisotropy energy, which drives alignment along specific crystallographic directions, and the exchange energy, which favors parallel alignment of neighboring moments.

The thickness of a domain wall is given by the expression:

$$\delta = \pi\sqrt{A / K} \qquad (1.2)$$

where A is the exchange stiffness constant, representing the strength of exchange interactions, and K is the anisotropy constant, quantifying the material's resistance to deviations from the easy magnetization direction.

II.3.6.2 Principle of Exchange Coupling

phenomenon of magnetic coupling between multilayers, particularly the exchange anisotropy resulting from this interaction, has been extensively studied both theoretically and experimentally. Exchange coupling plays a critical role in magnetoresistive devices, where achieving parallel and antiparallel configurations requires hardening one of the magnetic layers. The influence of structural properties on exchange coupling has driven significant research into the development and growth of magnetic layers.

Exchange coupling is an interfacial interaction occurring between a ferromagnetic (F) layer and an antiferromagnetic (AF) layer. This interaction induces anisotropy within the ferromagnetic layer, referred to as unidirectional anisotropy, due to the biasing field it creates. This field, known as the exchange field (He)), is illustrated in Figure 1.4 and is critical for determining the magnetic behavior of the F layer. Notably, (He) can reach magnitudes as high as 500 Oe .

The exchange field anchors the magnetization of the ferromagnetic layer along a preferred direction, termed the "easy axis" (EA), akin to traditional soft magnetic materials. Along this axis, the ferromagnetic layer often becomes saturated, mirroring the effect of an external magnetic field. Additionally, at 90° to the easy axis lies the "hard axis" (HA), characterized by the anisotropy field (Hk), a feature also observed in conventional soft magnetic layers. This dual-axis behavior underpins the functionality of magnetoresistive devices and highlights the importance of exchange coupling in modern magnetic technologies.

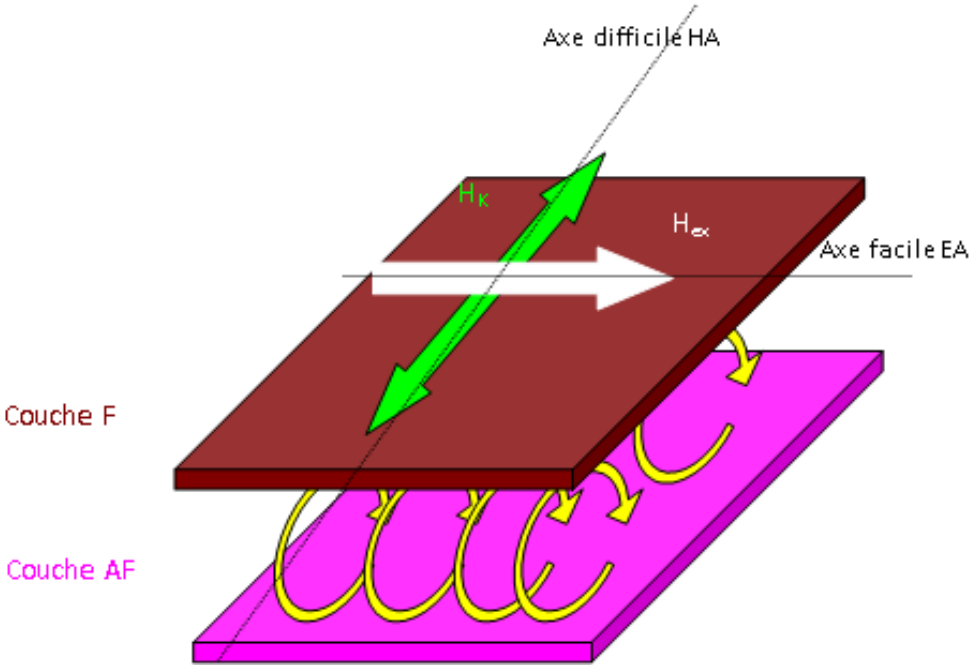

Figure 8: Schematic Representation of the Creation of Anisotropy Induced by Exchange Coupling Between an F (Ferromagnetic) Layer and an AF (Antiferromagnetic) Layer.

The exchange coupling results in a shift of the hysteresis loop along the easy axis corresponding to the value of the exchange field (Hex) and by a coherent rotation of the magnetization along the hard axis.

II.3.7 Mechanical Properties:

II.3.7.1 Hardness

The hardness of a metal is strongly influenced by its grain size—smaller grains result in harder materials. In conventional metals, structural defects called dislocations are present, which link aggregates. When stress is applied, these dislocations move, leading to deformation of the metal.

In contrast, nanomaterials contain significantly fewer dislocations compared to the abundance of grain boundaries and triple junctions. With these defects largely absent, the resistance to deformation becomes substantially higher, making nanomaterials harder than their polycrystalline counterparts.

Several theoretical models have been developed to describe the relationship between hardness, dislocations, and microstructural characteristics. The Hall-Petch model, introduced in the early 1950s, is foundational in this context. According to the Hall-Petch law, grain boundaries act as obstacles to dislocation movement, thereby enhancing the material's strength. In nanocrystalline materials, the reduction in grain size eliminates these boundaries as barriers, leading to increased hardness.

Other models, such as Cottrell's theory (1958), Li's model (1963), and Conrad's model (1963), further refine this understanding by linking hardness to factors like microstrain. These models suggest that, for a given crystallite size, hardness increases with higher rates of microstrains. Experimental studies have confirmed that the hardness of nanocrystalline metals and alloys prepared through mechanical grinding depends on both crystallite size and microstrain rate. During grinding, grain size decreases with time, while plastic deformation stress σ_p —the minimum stress required for plastic deformation—increases.

These observations align with the Hall-Petch relationship, which can be expressed as:

$$\sigma_p = \sigma_0 + \frac{K}{\sqrt{d}} \qquad \text{(Loi de Hall-Petch)} \qquad (2)$$

Where: σ_0 and k are constants depending on the material, and d is the sub-grain size.

When σ_p becomes greater than the stress applied during impacts, the latter is then insufficient to plasticize the material: the crystallite size then reaches a limit value, usually between 6 nm and 30 nm. This limit value depends on the nature of the ground material; in particular, for a pure metal, it is observed to be a monotonic function of the melting temperature. During grinding, when the limit grain size is reached, new interfaces (joints) can no longer form. For longer times, grinding leads to a disorientation of the grains relative to each other.

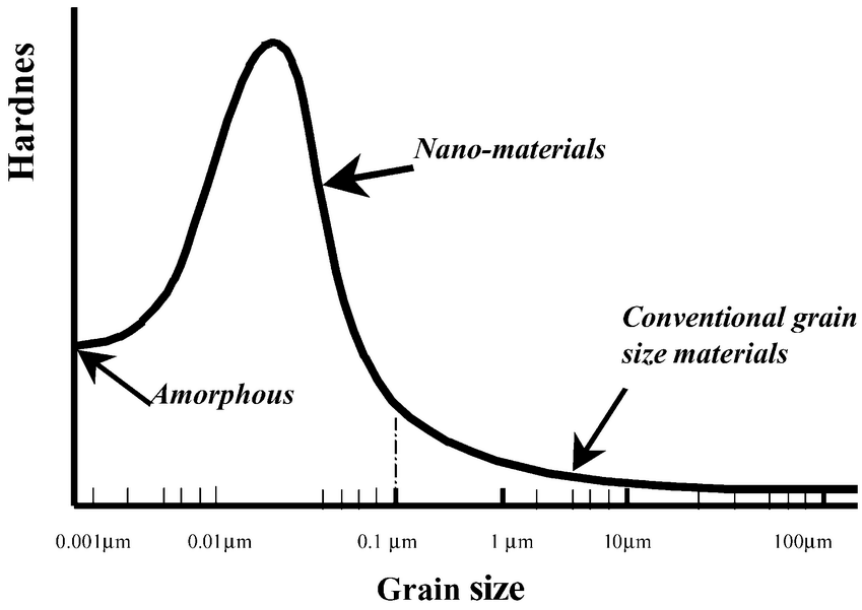

Figure 9: Effect of grain size on hardnes of materials

II.3.7.2 Ductility:

Nanomaterials offer a promising opportunity to combine high mechanical strength with enhanced ductility, a combination that can significantly expand their potential for applications requiring high formability or operation under stress. Achieving this balance, however, necessitates deliberate microstructural modifications in the prepared materials.

A key strategy involves tailoring the nature of grain boundaries to influence ductility. Grain boundaries in nanomaterials play a pivotal role in determining mechanical behavior, and optimizing their properties can enhance the material's ability to deform without fracturing.

Another effective approach is to introduce a bimodal distribution of grain sizes, where both coarse and fine grains coexist. This bimodal structure not only improves ductility but also helps delay the onset of necking, a critical factor in preventing premature material failure during deformation. Together, these microstructural adaptations enable nanomaterials to achieve a desirable combination of strength and ductility, unlocking new possibilities for advanced engineering applications.

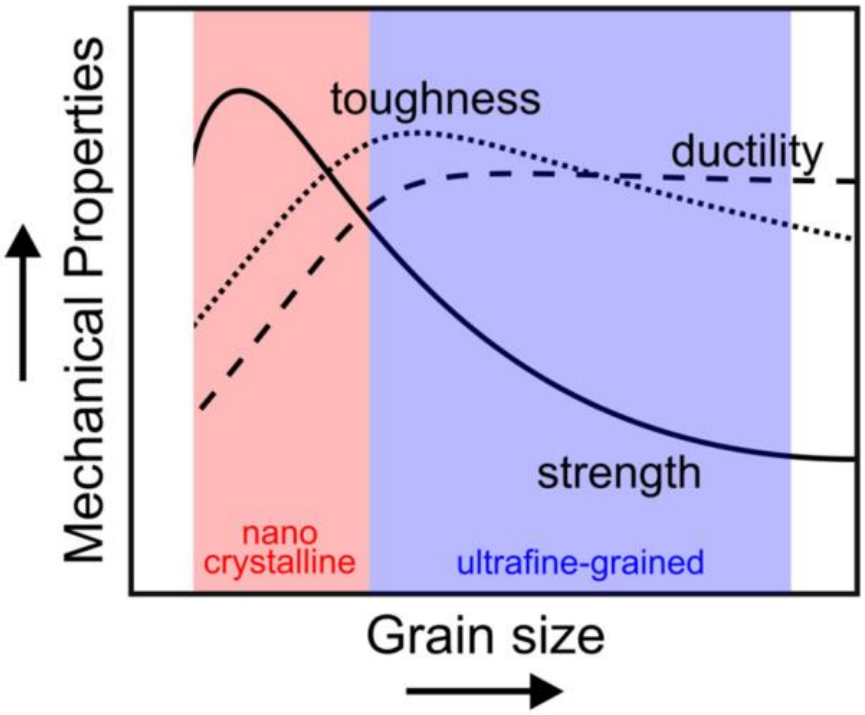

Figure 10: Machanical propreieties of nanomaterials

II.3.7.3 Malleability:

Malleability refers to a material's capacity to undergo deformation under compressive stress without fracturing. It is a measure of the material's ability to be shaped or formed, such as by hammering or rolling, without losing its structural integrity. Traditionally, materials exhibit a trade-off between hardness and ductility: a harder material tends to be less ductile, while a more ductile material often sacrifices hardness.

Nanomaterials, however, challenge this conventional trade-off. Materials composed of nanoparticles can simultaneously exhibit increased hardness and improved ductility due to their unique structural properties. For instance, nanoceramics, which are typically brittle in their bulk form, display enhanced malleability at the nanoscale. This is attributed to their refined grain structures and the significant influence of grain boundaries, which allow for better stress distribution and energy absorption during deformation.

The exceptional malleability of nanomaterials arises from their ability to undergo plastic deformation at smaller scales, where dislocations and defects are more easily accommodated or suppressed. This makes them both stronger and more adaptable than their conventional counterparts, enabling deformation without fracture under conditions where traditional materials would fail.

III. Synthesis of Nanomaterials

The methods for obtaining nanocrystalline materials can be classified according to the starting phase in the process. There are several techniques that, by their nature, can produce materials with small dimensions.

Among the techniques used in the production of nanocrystalline materials, we include:

- In the vapor state:

Physical vapor deposition, chemical vapor deposition, inert gas condensation, sputtering, plasma process, laser ablation.

- In the liquid state:

Electrodeposition, rapid solidification, sol-gel process.

- In the solid state:

Mechanical grinding, mechano-chemical synthesis, spark erosion.

To produce nanoparticles in large quantities, currently, only the recrystallization of amorphous ribbons and mechanical grinding appear to be feasible.

Nanostructured metal alloys can be obtained by high-energy grinding, flash sintering (SPS), SHS process (self-sustaining combustion), mechanically activated extrusion, high-pressure torsion, Electro-explosion of wire method (EEW), Ion beam milling, and Flash sintering (Spark Plasma Sintering (SPS)).

III.1 Physical Vapor Deposition (PVD) :

Physical Vapor Deposition (PVD) is a coating technique through vaporization that involves the transfer of material at the atomic level. The process can be described in the following sequence of steps.

(1) The material to be deposited is transformed into vapor by physical means (high-temperature vacuum or gas plasma),

(2) The vapor is transported from its source to the substrate in a low-pressure region,

(3) The vapor undergoes condensation on the substrate to form a thin film.

Typically, PVD processes are used to deposit films ranging from a few nanometers to thousands of nanometers in thickness.

However, they can also be used to create multi-layer coatings, graded compositions, very thick deposits, and self-supporting structures. A typical PVD process is illustrated in Fig. I.8.

PVD thin film technology encompasses a fairly wide range of deposition techniques, including electron beam or hot boat evaporation, reactive evaporation, and ion plating.

PVD techniques also include processes based on sputtering, whether by plasma or ion beam.

PVD is also used to describe deposition from arc sources, which may or may not be filtered.

In general, this process can be divided into two groups: evaporation and sputtering. Evaporation refers to the deposition of thin layers by thermal means, whereas in sputtering, atoms or molecules are dislodged from the solid target by the impact of

gaseous ions (plasma). Both methods have been developed into several specific techniques.

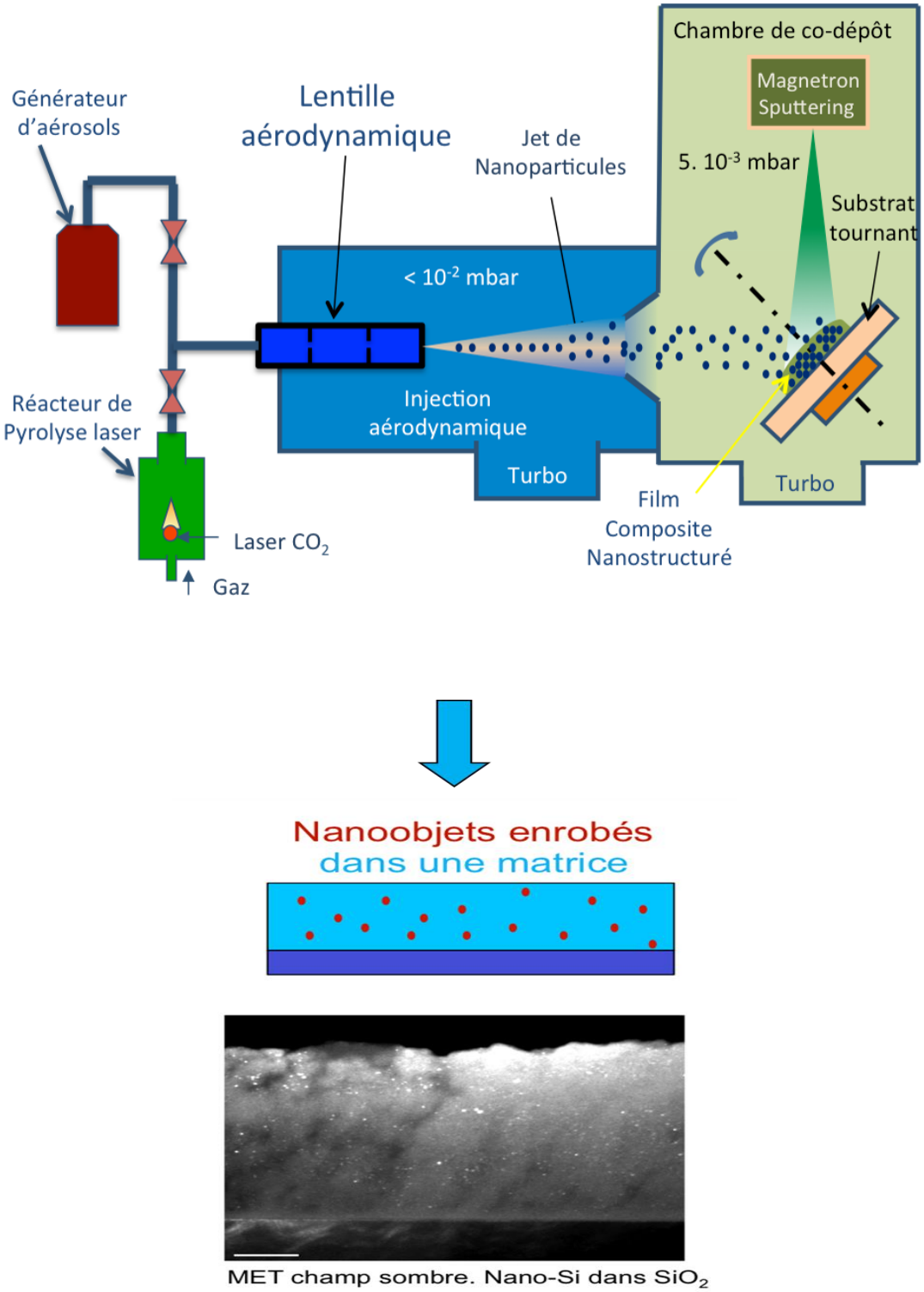

Figure 11 : Physical Vapor Deposition (PVD) processes

III.2 Inert Gas Condensation

The inert gas evaporation method has been extensively utilized by the Japanese school since the 1960s, and in 1991, Uyeda published an excellent and comprehensive summary of the Japanese literature on the topic.

It has been demonstrated that a wide variety of metals with very fine particles can be synthesized in a low-pressure inert gas atmosphere, and their sizes can be controlled by varying the gas pressure (in the range of 1 to 30 Torr).

Inert Gas Condensation (IGC) is a bottom-up approach for synthesizing nanostructured materials, involving two basic steps. The first step involves the evaporation of the material, and the second step involves rapid, controlled condensation to produce the required particle size.

In this process, the chamber is evacuated to a pressure of about 2×10^{-6} Torr using an oil diffusion pump. The crucible containing the metal to be evaporated is slowly heated by radiation from a graphite heating element.

The temperature is set to a predetermined value. After evacuation, an inert gas (He, Xe, or Ar) is introduced into the chamber at low pressure, typically around 0.5–4 Torr, and the crucible is quickly heated (at constant inert gas temperature and pressure).

The ultrafine metal particles that nucleate and grow in the gas phase are collected on a water-cooled surface.

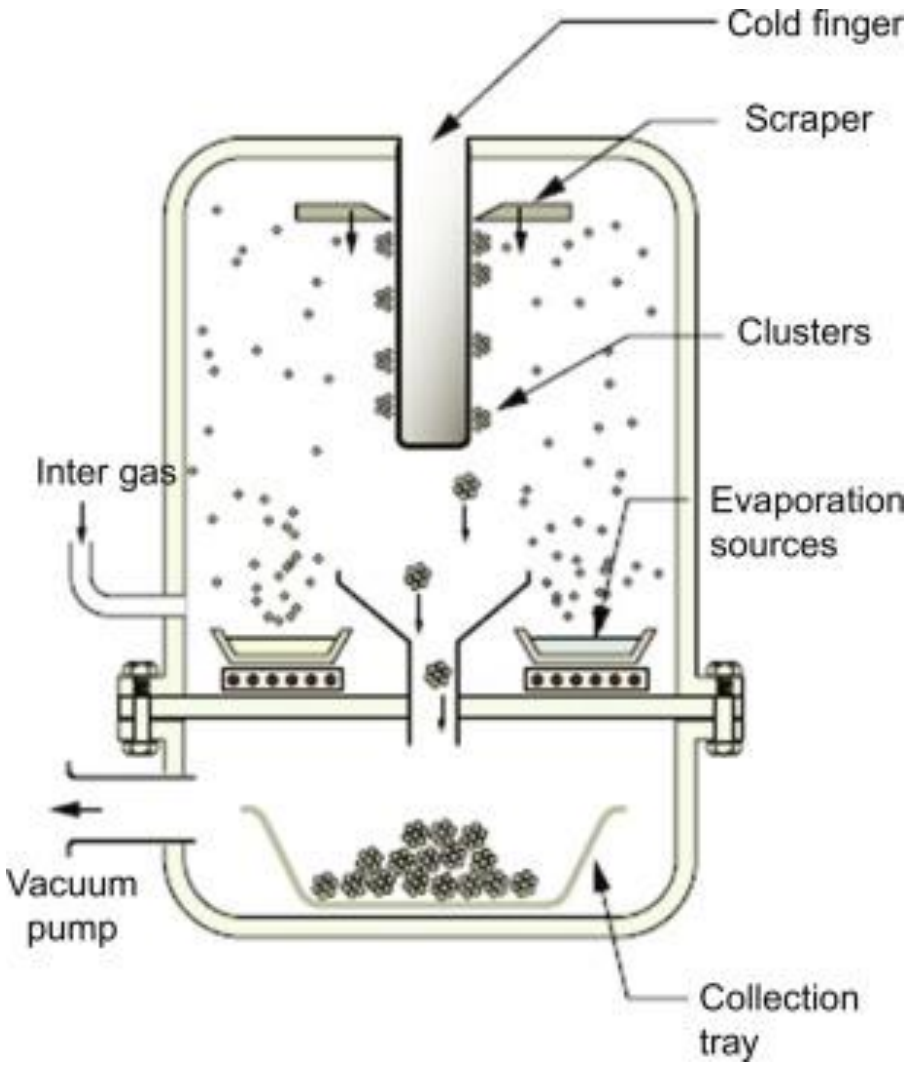

Figure 12: Schematic representation of an inert gas condensation chamber for synthesizing nanostructured materials.

Using a shutter mechanism, it is possible to extract samples with a thickness less than a single particle layer from the grid. Figure 12 provides a detailed schematic of a modern apparatus commonly employed for this purpose.The core components of this apparatus retain similarities to those originally utilized by Granqvist and Buhrman. However, the design has been enhanced with two significant advancements:

1. A scraper system designed to efficiently collect powder particles into a designated container, ensuring streamlined handling and storage.

2. An integrated mechanism enabling **in situ** compaction of bulk powders, which facilitates the direct consolidation of materials within the chamber itself.

These modifications not only improve the efficiency of the synthesis process but also expand the functional versatility of the equipment, making it suitable for advanced applications in nanotechnology.

III.3 Spray Conversion Processing

Spray conversion processing consists of three sequential steps. In the first step, an aqueous solution of the precursor compound is prepared and mixed to fix the composition of the starting solution. In the second step, the starting solution is spray-dried to form a chemically homogeneous precursor powder. In the final step, the precursor powder is thermochemically converted into the desired nanostructured final product powder. A schematic illustration of this process is presented in Fig. 12.

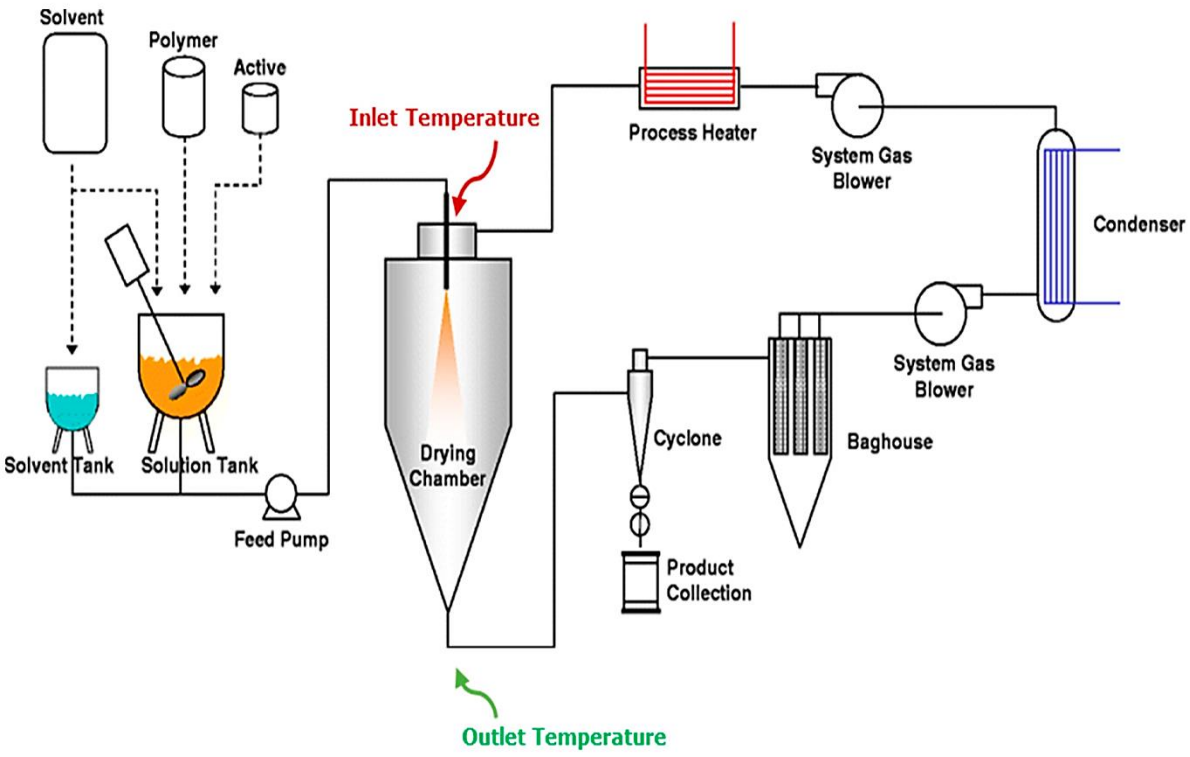

Figure 13: Diagram of the Spray Conversion Process, developed by Nanodyne

The final step can be carried out in a fixed-bed reactor when the quantity of powder treated is low, but for the thermochemical treatment of large quantities of powder, it is advisable to use a fluidized bed reactor to ensure a uniform conversion rate for all particles in the bed. The three stages of the process are easily scalable.

Spray drying is an essential step in the process when dealing with starting solutions containing two or more precursor compounds. The rapid drying of aerosol droplets, accompanied by rapid solute precipitation, produces a chemically homogeneous precursor powder even from a complex starting solution.

In other words, spray drying tends to eliminate the phase separation that normally occurs during the conventional crystallization of the solution mixture.

Typically, spray-dried precursor particles are spherical shells about 10 to 50 μm in diameter and have amorphous or microcrystalline structures.

Thermochemical conversion of the precursor powder in fluidized bed reactors is also an important step of the integrated process. This is due to the fact that the local temperature and gas concentration environment in the fluidized bed reactor is the same for all parts of the bed, ensuring uniform conversion of the precursor powder into the final product powder. This is not the case for fixed-bed reactors where uniformity

III.4 Chemical Vapor Condensation

A modification of the conventional IGC system, called chemical vapor condensation, was used to synthesize silicon-based ceramics in 1994.

A diagram of the apparatus is illustrated in Fig.14. Gas flow is introduced at a controlled rate into the dynamic pumping vacuum chamber through a needle valve. The pressure in the chamber is maintained at a constant low pressure (1–50 mbar) by high-speed pumping.. The high purity Al2O3 tubular heater provides a heat source for the controlled decomposition of the precursor.

During the short residence time of the precursor in the heated tube, the individual precursor molecules begin to decompose and combine to form small clusters or particles.

At the reactor's exit, the rapid expansion of the cluster or particle beam serves to mitigate growth and agglomeration of particles. Finally, the particle beam condenses on a rotating substrate cooled with liquid nitrogen from which the powders can be scraped and collected.

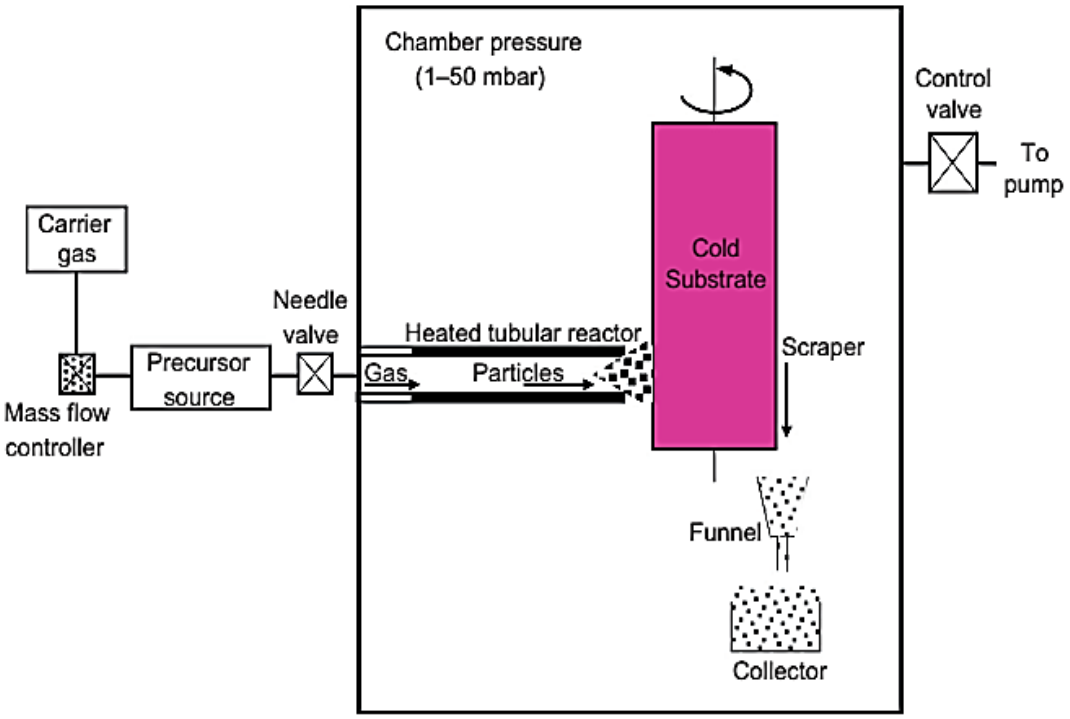

Figure 14: Sschematic of the chemical vapor condensation system.

III.5 Top-Down Methods

As mentioned earlier, the top-down approach starts from a bulk material that incorporates critical details at the nanometer scale. In this method, a material is engineered by breaking down a complex entity into its parts, such as creating small crystals from a hard, mineralized bulk tissue. This type of fabrication relies on a number of tools and methodologies, which consist of three main steps:

1. The deposition of thin films/coatings on a substrate;

2. Achieving the desired shapes through photolithography;

3. Pattern transfer using either a lift-off process or selective etching of the films. Below, some methods of the top-down approach are described.

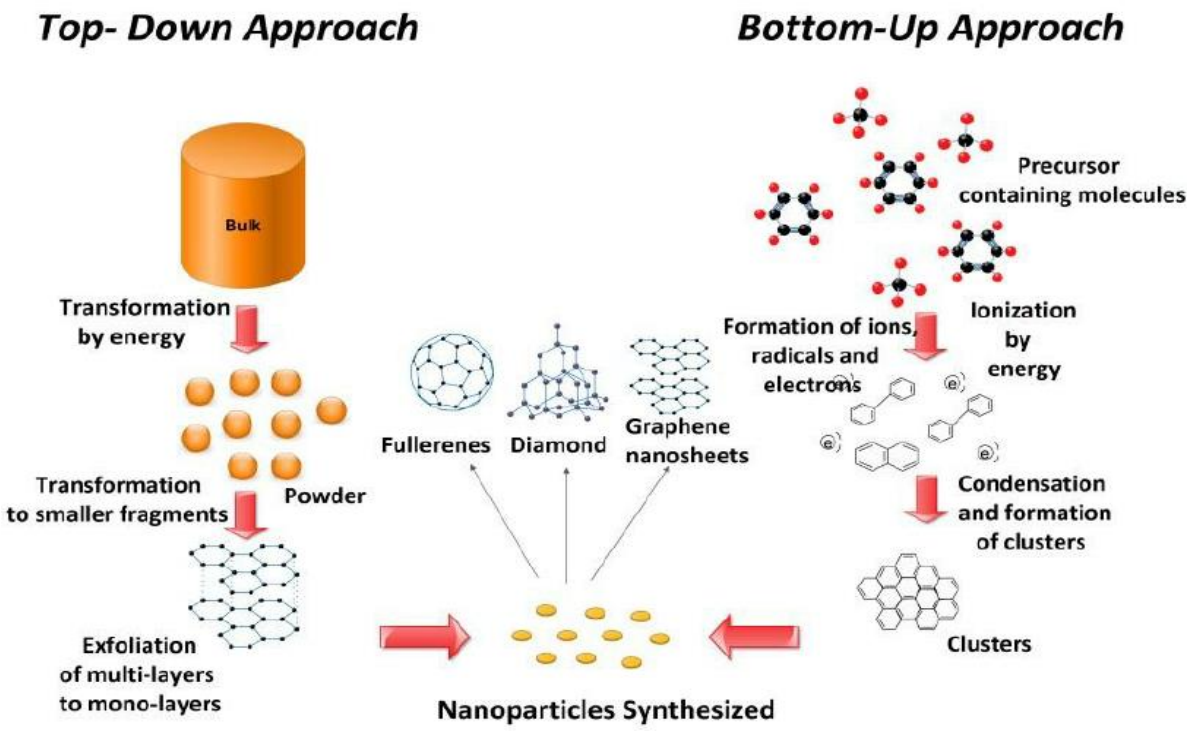

Figure15: Bottom-Up and Top-Down Approaches in the Synthesis of Carbon-Based Nanomaterials

III.6 Sputtering:

Cathodic sputtering is one of the most important PVD techniques in which the physical vaporization of atoms from a surface occurs by momentum transfer from bombarding particles that are energetic and atomic-sized. Sputtering deposition allows for better control over the composition of multi-element films and greater flexibility in the types of materials that can be deposited.

Although first reported by Wright in 1877, the deposition of films by sputtering became feasible only due to the relatively low vacuum required for its operation. Despite the fact that Edison patented a cathodic sputtering deposition process to deposit silver on wax photographic cylinders in 1904, the process was not widely used in the industry until the advent of magnetron sputtering in 1974.

The application of cathodic sputtering deposition led to an acceleration in development, from reproducible, stable, and long-lived vaporization sources for production purposes. Following the use of a magnetic field that confines the movement of secondary electrons near the target surface, planar magnetron sputtering has become the most widely used sputtering configuration.

It was originally derived from the development of the microwave klystron tube during World War II, research by Kesaev and Pashkova (in 1959) on confinement arcs, and Chapin's (in 1974) development of the planar magnetron sputtering source. The operating principles of direct current and radiofrequency sputtering systems are schematically illustrated in Fig. 16. Effective cathodic sputtering deposition can be achieved in:

- A good vacuum (,10^{-25} Torr) using ion beams;

- A low-pressure gaseous environment, where the sputtered particles are transported from the target to the substrate without gas-phase collisions (i.e., a pressure lower than about $5x10^{-3}$ Torr), using a plasma as the ion source;

- A high-pressure gas, where gas-phase collisions occur.

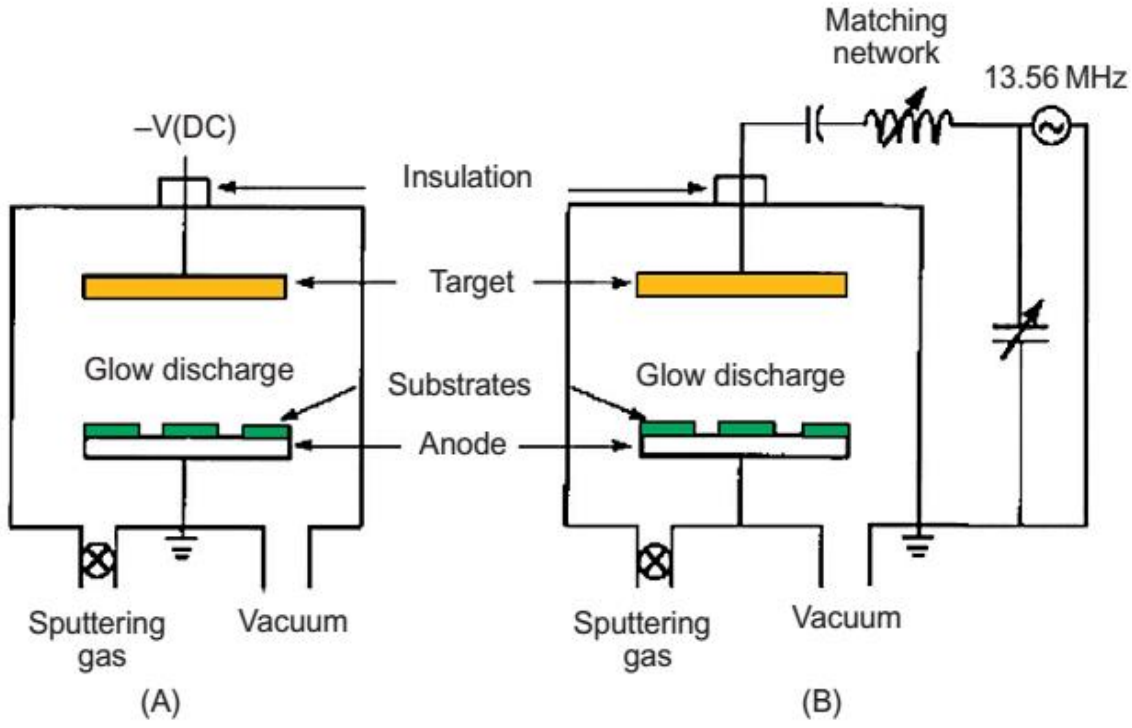

Figure 16: Schematic Diagram of Sputtering Systems (A) DC (Direct Current) and (B) RF (Radio Frequency).

Currently, plasma-based sputtering is the most common form of sputtering in which a plasma is present and positive ions are accelerated towards the target, which is at a negative potential relative to the plasma. At higher pressures, ions undergo physical collisions and charge exchange collisions, resulting in a spectrum of energies of ions and neutrals bombarding the target surface. At lower pressures, ions reach the target surface with energy given by the potential drop between the surface and the point in the electric field where ions are formed. In vacuum cathodic sputtering, however, an ion or plasma beam is formed in a separate ionization source, and is then accelerated and extracted into a treatment chamber that is maintained in good vacuum conditions. In this process, the average bombardment energy is higher than plasma-based bombardment, and the high-energy reflected neutrals are more energetic.

Cathodic sputtering deposition can be used to deposit films of elemental materials, as well as to deposit alloy films and maintain the composition of the target material. This is possible because the material is removed from the target layer by layer, which is one of the main advantages of the process. This allows for the deposition of some quite complex alloys such as Al Si Cu for semiconductor metallization and Cr Al Y metal alloys for coatings on aircraft turbine blades.

Film deposition of composite material by sputtering can be achieved by sputtering from a composite target or by sputtering from an elemental target at the partial pressure of a reactive gas (i.e., "reactive sputtering"). In most cases, cathodic sputtering deposition of a compound material from a composite target results in a loss of some of the more volatile material (e.g., oxygen from SiO2). However, this loss is often compensated by deposition in an atmosphere containing a partial pressure of the reactive gas - a process known as "quasi-reactive sputtering". In the latter case, the required partial pressure of the reactive gas is lower than the partial pressure used for reactive sputtering.

However, the above techniques are often limited to the fabrication of small-scale specimens commonly used in electronic devices but are generally not suitable for large-scale structural applications. Furthermore, the finished products from these techniques invariably contain residual porosity and contamination. According to recent studies, large bulk metals in a fully dense state can be manufactured by combined cryo-milling, hot isostatic pressing, and subsequent extrusion. However, this method is costly and not easily adaptable to structural alloys used in large-scale industrial applications. The "top-down" approach is different as it depends on taking a bulk solid with a relatively coarse grain size and processing the bulk solid to produce ultra-fine grain and nano-grain microstructures through severe deformation. This approach avoids the small product sizes and contamination that are inherent features of materials produced using the "bottom-up" approach, and it has the additional advantage that it can be easily applied to a wide range of preselected alloys.

III.7 High-Energy Milling

High-energy mechanical grinding, also known as mechanosynthesis, was developed in the 1960s by John Benjamin to achieve dispersions of oxides (Al2O3, Y2O3) in nickel alloys to enhance their mechanical properties. Mechanical milling has a fairly broad application potential. It allows for the achievement of unique structures with low development costs. This is why it experienced a real boom in the 1980s and 1990s. Since then, it has been expanded to the development of a variety of stable and metastable phases: solid solutions, crystalline and quasi-crystalline phases, intermetallics, amorphous alloys.

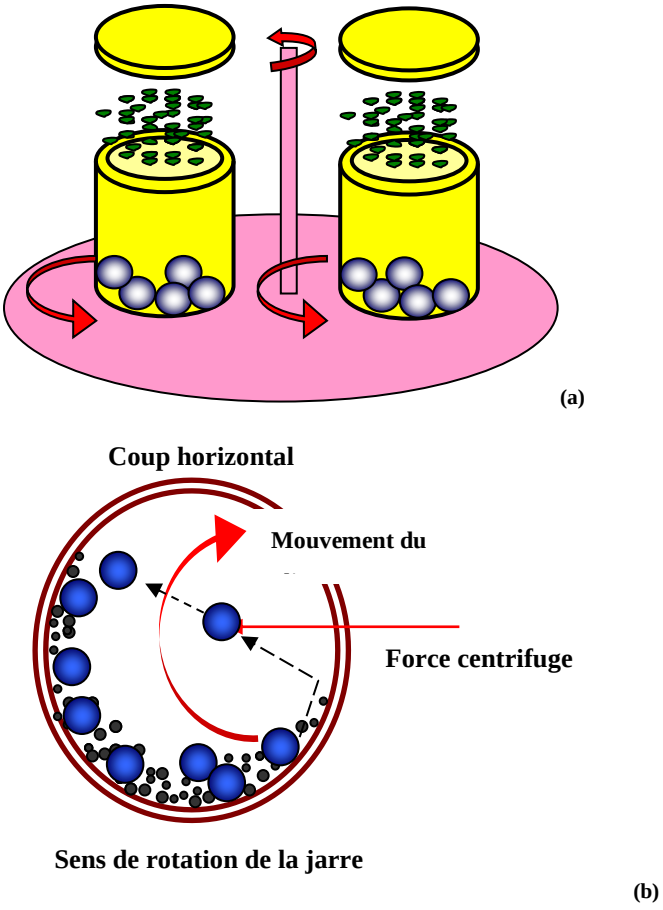

Figure 17: Operating Principle of the Planetary Mill:

(a) Rotation of the jars in relation to the platform.

(b) Movement of the balls inside the jars.

III.7.1 Principle

Mechanical milling is a very powerful technique for mixing powders of pure elements or combinations achieving atomic scale. The synthesis process through milling has been described as a succession of events during which powder particles are welded, fractured, and rewelded. This leads to an extremely fine intimate mixture with the possibility of forming a variety of equilibrium and non-equilibrium phases including supersaturated solid solutions, intermediate crystallized and metastable phases, and amorphous phases. Materials elaborated by mechanical milling are characterized by a submicron grain size matrix. Nanosize reinforcements (borides, oxides, carbides, etc.) can be introduced into the material either by direct addition of ceramic powder or by reaction with an additive. The role of the dispersoids is to prevent grain growth at high temperatures.

The reduction of material into small fragments or powder is achieved through the operation of milling. The mechanisms are far from clear, and we have chosen to use the theory of mechanical fracture to explain the fracture of particles subject to mechanical forces. Classic fragmentation modes consist of subjecting the solid to be fragmented to a stress created by contact forces. The resulting stress field is generally anisotropic and depends on parameters intrinsic to the material, the number and direction of forces, and the rate of deformation. The technology of devices takes into account the following parameters:

- Material's intrinsic parameters: They determine its behavior during deformation.

- The stress field applied to the solid affects discontinuities for the initiation and propagation of cracks, whose distribution determines the size, shape of fragments, and the new surfaces created.

- Energy required to fracture the material: It is released by the stress field. The energy needed for rupture is additional energy because crack propagation consumes

energy. It is proportional to the grain's cross-section, while stored energy is proportional to volume.

- Deformation rate: It conditions the material's behavior.

- Reduction in material dimensions: It is not unlimited and most of the time requires successive stages involving different types of devices working in series.

Generally, three types of fragmentation are distinguished:

1. Coarse fragmentation;
2. Fine fragmentation;
3. Ultrafine fragmentation.

Each type of fragmentation corresponds to specific apparatus and particular fragmentation mechanisms. We have focused only on fine and ultrafine fragmentations and their different types of apparatus. This technique consists of milling two materials, A and B, together. Initially, there is a fragmentation phenomenon of particles from different constituents (Fig. II.4) until a limit size is reached. One of the constituents fragments much more rapidly, here constituent B. Thus, B reaches its limit fragmentation size before A.

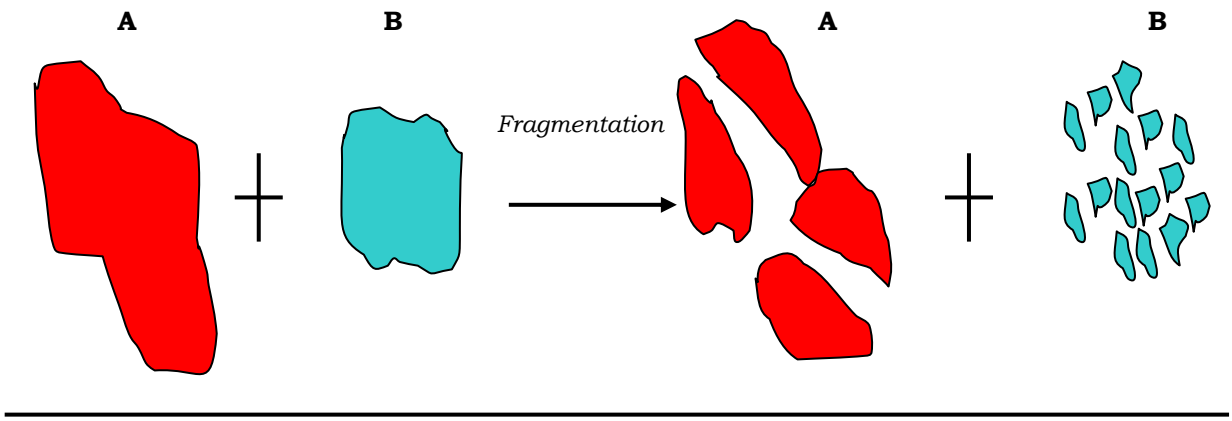

Figure 18: Diagram of the Fragmentation Phenomenon During Milling.

The fine particles of constituent B, due to inter-particle forces, tend to stick to the larger particles. The longer the milling continues, the more this phenomenon amplifies. Different stages of agglomeration will be encountered: the simple welding between two or more particles, then the coating stage of particles, and finally the agglomeration stage of particles among themselves. The type of phenomenon observed will depend, among other things, on the duration of the operation and the affinity of the products. Figure 18 shows the evolution of the different agglomeration stages during milling.

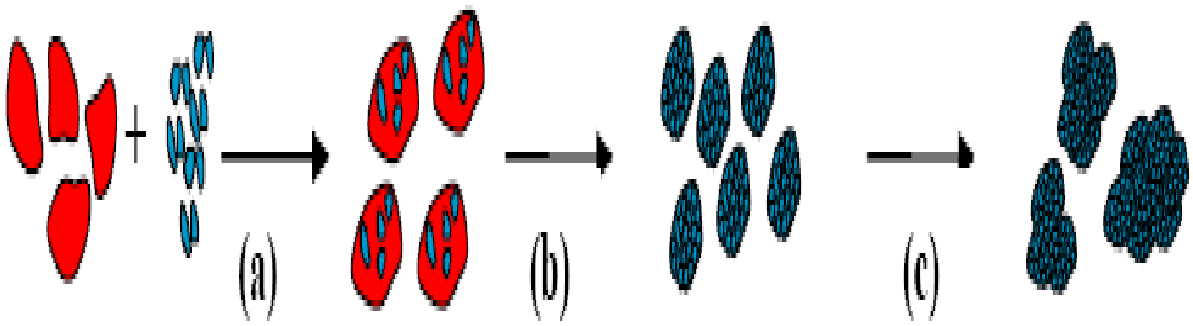

Figure 19: Different Stages of Agglomeration During Milling:

(a) welding, (b) coating, and (c) agglomeration.

During high-energy milling, the powder particles trapped between balls or between the balls and the jar wall are subjected to plastic deformations, accompanied by hardening phenomena and local temperature increases. They are fractured, and the

fragments are then welded back together. Typically, around 1000 particles with a cumulative weight of about 0.2 mg are trapped during each collision (Fig. 18).

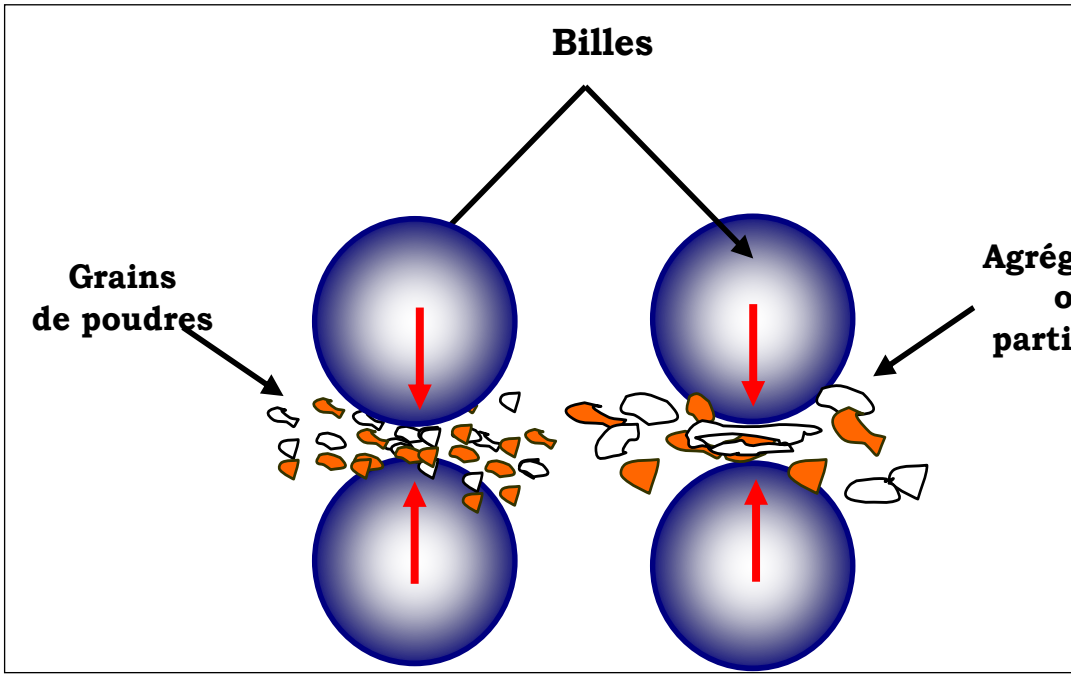

Figure 19: Principle of Mechanical Milling: Formation of Aggregates by Mechanical Impacts.

III.7.2 Experimental Conditions of Milling

III.7.2.1 Nature of the Powders:

Due to the continuous impact of the balls, the particle structure is refined, but the particle size continues to be identical. Consequently, the interlayer spacings decrease, and the number of layers in a particle increases. There are three types of starting mixtures that have been described: ductile-ductile systems, ductile-brittle, and brittle-brittle.

III.7.2.1.1 Ductile – Ductile System:

For Benjamin, the ideal combination of materials in mechanical milling suggested that there needed to be at least 15% of a malleable component to achieve the alloy. This was because true alloying occurs due to the repeated action of fracture and welding of powder particles; welding cannot occur if the particles are not ductile. Initially, the particles flatten and form lamellar structures that weld together. These structures are then fragmented by the continuation of milling, and the thickness of the lamellae decreases. After sufficiently long milling, the achieved mix becomes atomic in order.

III.7.2.1.2 Ductile – Brittle System:

The ductile compound is rolled, and the brittle compound is fragmented in the first step, followed by the incorporation of the brittle compound between the lamellae of the ductile compound. With the continuation of milling, this mixture is fragmented, followed by a uniform distribution of the brittle compound in the ductile matrix, and finally, it is possible to achieve a mix at the atomic level (a true alloy or an intermetallic compound).

III.7.2.1.3 Brittle – Brittle System:

Normally, these powders cannot be alloyed by mechanical milling, but under the influence of temperature, it is possible to perform thermal activation accompanied by a reduction in particle size when the less brittle powder can behave like ductile materials (fragmentation limit). When one constituent becomes ductile, the process occurs as for the brittle – ductile system.

III.7.2.2 The Mill:

All types of mills consist of one or more jars in which balls or rods are contained that act on the materials placed in the jar in powder form. The jars and balls (or rods) are generally constructed of materials that exhibit strong resistance to wear and to avoid contamination. Milling is usually performed under a controlled atmosphere (argon,

nitrogen, etc.) in different types of mills classified according to the mode of action on the jar and/or ball. For example, the following mills can be cited:

III.7.2.2.1 The Attritor:

It consists of a chamber in which a vertical pestle, to which bars are attached perpendicularly at 90° to each other, drives balls in motion. The capacity of an attritor ranges from 0.5 to 40 kg of powder, but the energy provided to this powder is low. The attritor is a low-energy mill.

Figure 55: The low-energ attritor is a y mill

III.7.2.2.2 The Vibratory Mill:

It consists of a jar containing balls. The jar is moved horizontally forward, backward, and laterally with a frequency of about 20 Hz (e.g., Spex 8000 model). The capacity of this type of mill is a few tens of grams of powder, but the impact speed of

the balls is of the order of m/s and the shock frequency of the order of hundreds of Hz. The vibratory mill has the highest energy among the mills used for milling.

Figur 56: The vibratory mill

III.7.2.2.3 The Planetary Mill:

In this mill, about ten balls of 1 or 2 cm in diameter are placed with the powder in a jar, which is attached to a disc that rotates in the opposite direction to it. The milling acts either by impacts or by friction. Without external heating, the average temperature of the jar ranges from 50°C to 120°C, depending on the speed of the balls, with local temperature rises ranging from 60 to 300°C. To avoid excessive heating, milling is generally carried out in several cycles interrupted by rest periods. The steady state is stabilized after 24 to 100 hours of milling, depending on the materials milled. And this type of mill was used in our research.

Figure 20: Fritsch Pulverisette Planetary Mill

III.7.2.2.3.1 Grinding Intensity:

It depends on the type of mill. Indeed, the higher the energy, the faster the final product is obtained. There are certain limitations to the maximum intensity depending on the type of mill. In a conventional mill, increasing the rotation speed leads to an

increase in the movement of the balls. Also, intensive grinding promotes an increase in the temperature of the jar, which is advantageous in some cases where diffusion is required for homogenization and/or intimate mixing of powders. However, in some cases, the increase in temperature accelerates the transformation process and results in the decomposition of supersaturated solid solutions or other metastable phases formed during grinding. Similarly, a transformation from an energetically stable state to a metastable state can be achieved by grinding at relatively low speeds. This is the case for transformations: crystalline to quasi-crystalline, crystalline to amorphous, and quasi-crystalline to amorphous. Transitions from one phase to another can be favored by further grinding at high or low speed. Eckert et al. studied the influence of grinding intensity (I = 3, 5, 7, and 9) on the amorphization of the Al65Cu20Mn15 mixture. They showed that intensity I = 5 leads to the formation of an amorphous phase after 30-600 minutes of grinding, while intensity I = 9 favors the formation of the nanocrystalline CsCl-type phase. The estimated maximum temperatures are of the order of 520 K and 863 K for I = 5 and 9, respectively.

III.7.2.2.3.2 Grinding Time:

It is the parameter that describes the time interval needed to obtain the final product. It depends on the type of mill, the mode of action of the balls on the powder (elastic collisions or friction), and the grinding temperature. For example, grinding the Co80Ni20 powder mixture in a planetary mill under different conditions is completed after 3 and 48 hours of grinding for the samples. The effect of grinding conditions is more pronounced in the case of the mixture, and the final product is different.

III.7.2.2.3.3 Ball-to-Powder Weight Ratio (BPR):

It influences the formation of phases in the ground powders. It can vary from 1/1 to 220/1. With the increase of this ratio, it is possible to reduce the time needed to obtain the final product. Thus, the larger the ratio, the higher the number of collisions per unit of time, which leads to an increase in local temperature, and consequently, the

grinding process would be faster. The energy transfer to the powder depends on the number and diameter of the balls.

III.7.2.2.3.4 Grinding Atmosphere:

It can influence the nature of the final product and its size. In general, inert gases (Ar, He) are used to avoid contamination, but also air, nitrogen N2, or hydrogen H2, to produce oxides, nitrides, and hydrides. Inert gases can create defects and be "trapped" in the final compound. Depending on the nature of the atmosphere, grinding can be performed in a dry environment (air, Ar, He, N2, or H2) or wet (organic compounds can be introduced, for example, into the inert gas atmosphere).

III.7.2.2.3.5 Grinding Temperature:

It has an influence on the process of forming the final product. A high temperature favors the increase of the crystallite size but reduces their strains and solid-state solubility. There is a difference between the temperature of the balls and that of the jar wall as well as between that of ductile and brittle powders. However, excessive temperature increase accelerates the transformation process and the decomposition of solid solutions or metastable phases formed during grinding or even the mechanical recrystallization of the amorphous phase.

III.8 Spark Plasma Sintering (SPS):

SPS is a process similar to conventional hot pressing as the precursors (usually without sintering additives) are also introduced into a chamber allowing the application of uni-axial pressure during sintering. In the majority of cases, this chamber consists of a sheath and pistons made of graphite (figure II.7) but can also be made of steel or ultra-hard carbide (such as WC-Co). The use of specific graphite for the sheaths allows reaching consolidation temperatures of about 2000°C and uni-axial pressures up to 200MPa. However, the use of steel or Carbide matrices will limit the sintering temperatures to 500°C and 700°C, respectively. Sintering is generally carried out under secondary vacuum, but it can also be done under a neutral

Atmosphere (Argon, Nitrogen...), reducing (hydrogen) or even under an oxidizing atmosphere, but in this last case, graphite sheaths are to be avoided.

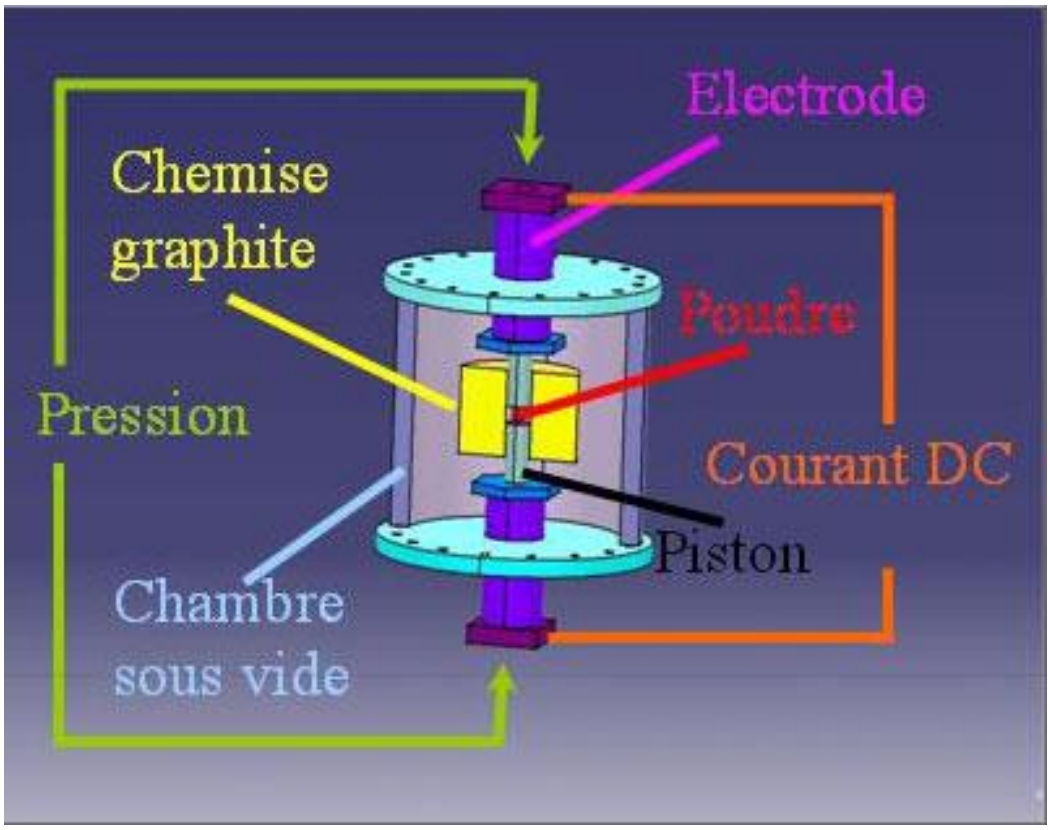

Figure 21: Principle Diagram of Spark Plasma Sintering

III.9 SHS Process (Self-propagating High-temperature Synthesis) (self-sustained combustion)

The principle of the SHS process (an acronym for Self-propagating High-temperature Synthesis, the name most often given to the process) has been known for a long time. An SHS-type reaction involves intimately mixing the reactants (usually in powder form), optionally compacting them, and then initiating the reaction with a sudden and localized energy input. Due to its highly exothermic nature, the reaction propagates until the complete consumption of reactants (figure 22). Thus, there is an analogy with the description of classical combustion, the most significant difference being the solid nature of the final product. It is the added value of this product, not the production of heat, which justifies the reaction. The process is often called "combustion synthesis" and sometimes "solid flame."

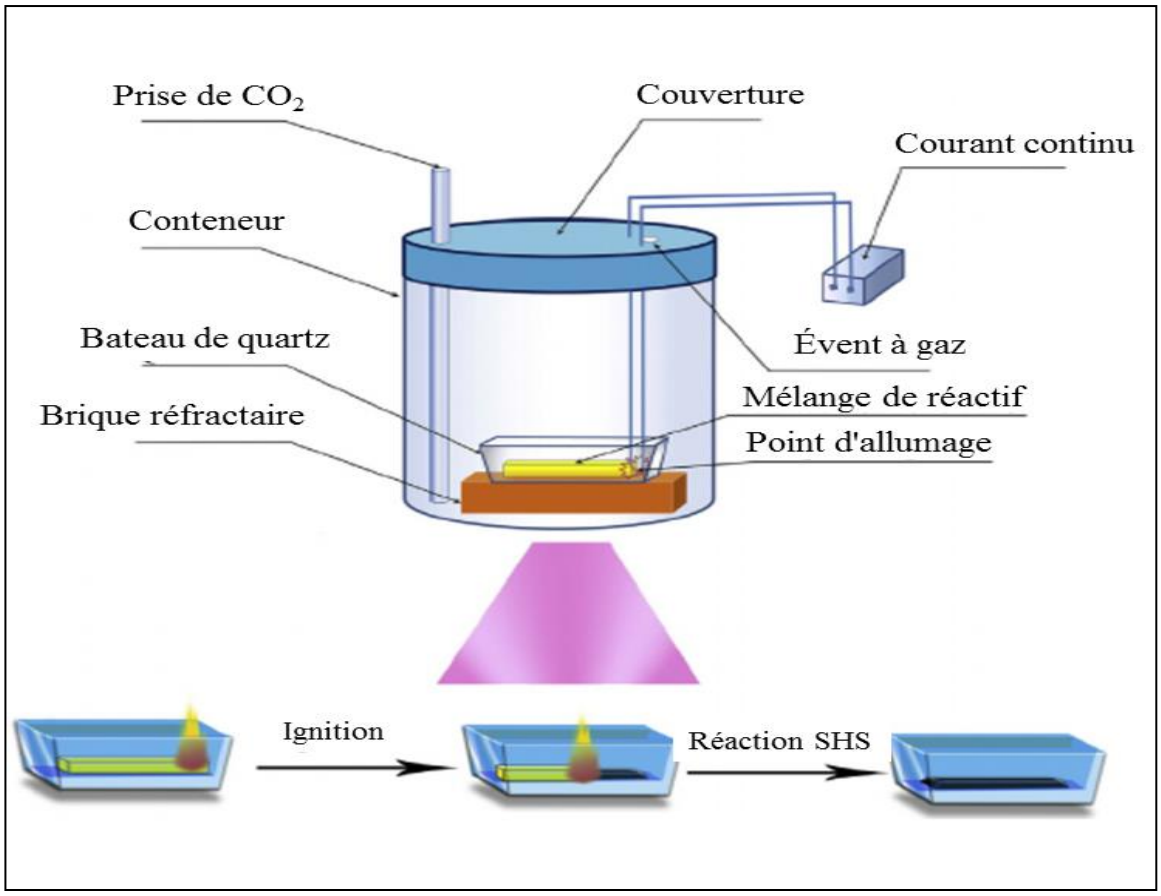

Figure 22: Diagram of the SHS Process (Self-propagating High-temperature Synthesis)

III.10 High-Pressure Torsion

III.10.1 Deformation by torsion under high pressure

The sample is placed in a chuck, and pressure is applied to the piston that enters the chuck's cavity. As a result, there is a significant frictional force between the two faces of the sample and the tool. The piston is rotated around its axis to cause torsional deformation of the sample (figure 23), subjecting the sample to significant radial shear.

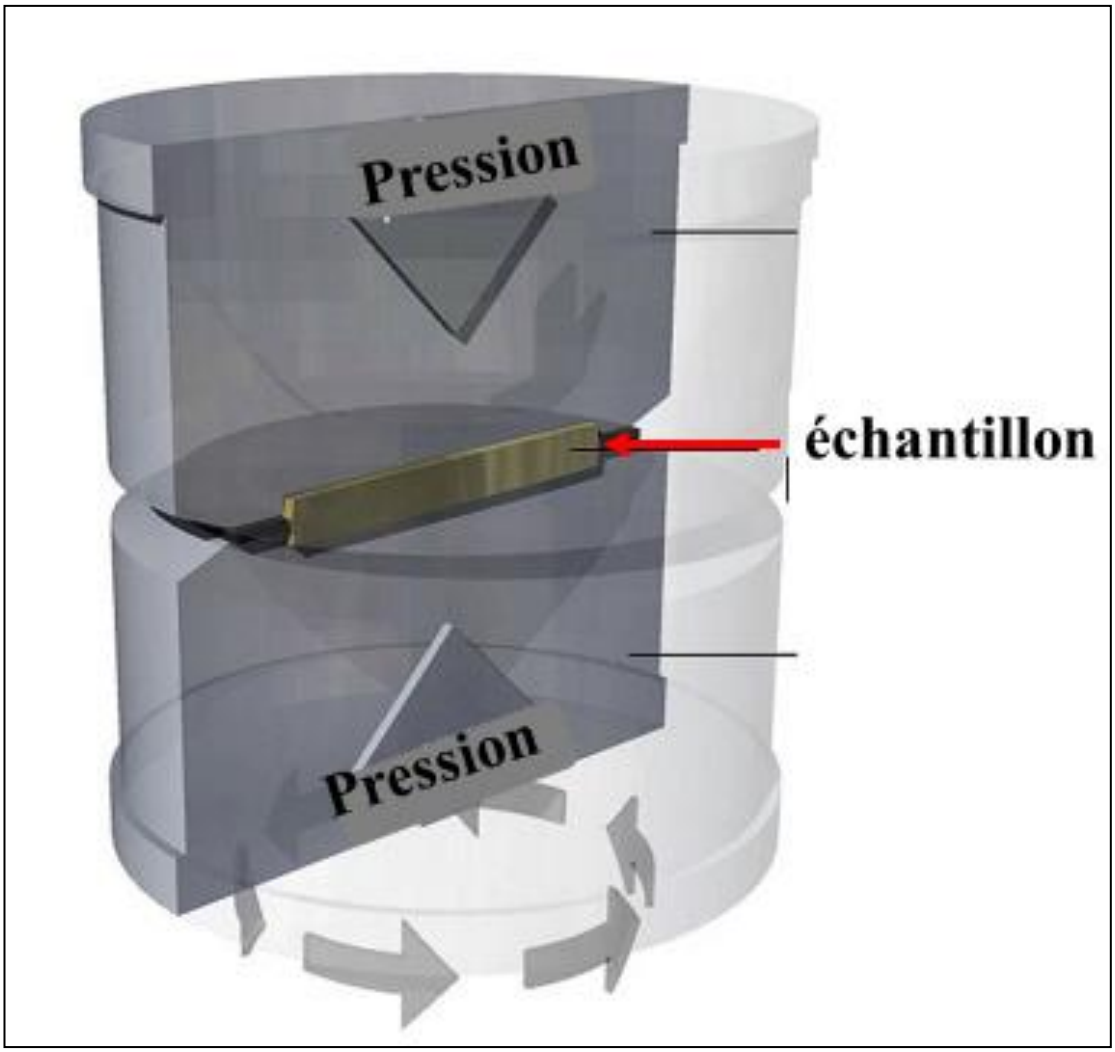

Figure 23: Deformation by High-Pressure Torsion

The use of this process in powder metallurgy leads to a significant reduction in porosity, which is advantageous. However, the disadvantages of this technique include:

- Limited shape and size of samples (discs of 10 to 20 mm in diameter and a thickness of 0.2 to 0.5 mm);

- Non-uniform distribution of deformation (low at the core but increasing along a radius of the cylinder).

III.10.2 Equal Channel Angular Pressing (ECAP)

The technique, schematized by Figure 24, allows the introduction of significant deformation by passing a sample through two channels of constant cross-section that are misaligned by an angle Φ. The deformation is imposed by means of a piston to which a pressure P is applied. The obtained microstructure is influenced by the number

of passes and the misalignment between the channels. The yield limit and mechanical strength increase simultaneously with the number of passes. Again, the samples are limited in size: 70 to 100 mm long with a diameter of less than 20 mm.

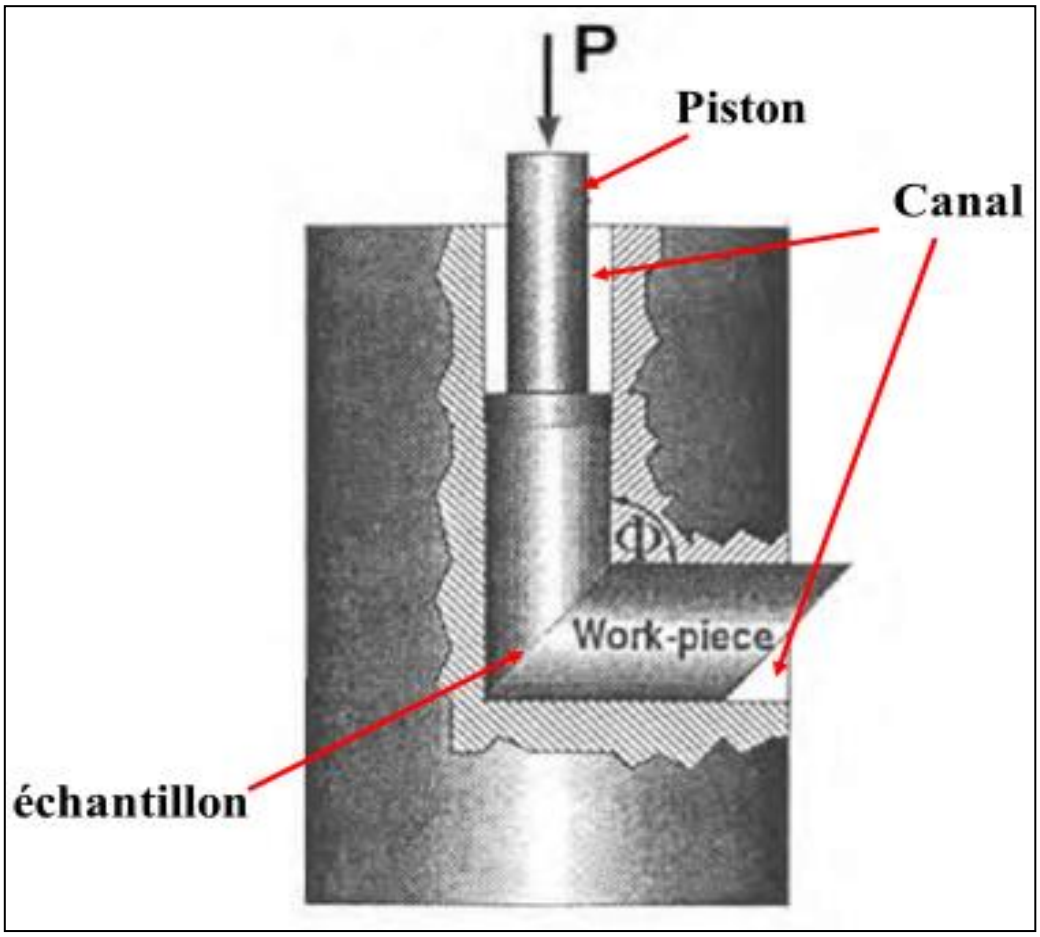

Figure 24: Equal Channel Angular Pressing (P is the applied pressure; φ is the angle between the channels).

III.11 The Electro-Explosion of Wire Method (EEW):

During the electro-explosion of a wire, particles are produced by evaporating a thin metallic conductor subjected to a high current under an inert atmosphere. The basic setup for wire explosion is shown in Figure 25.

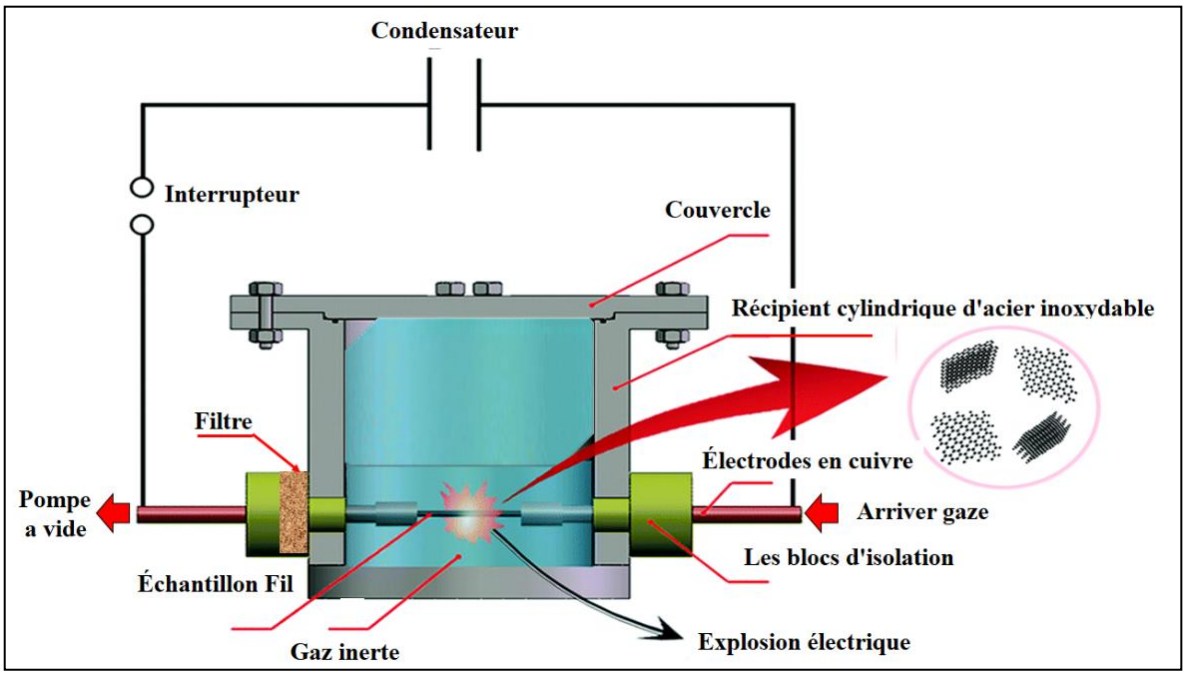

Figure 25: Diagram of the Electric Explosion Chamber

1 - lid, 2 - stainless steel cylindrical container, 3 - copper electrodes, 4 - insulation blocks, 5 - distilled water, 6 - high purity graphite rods

- The capacitor is charged, and the wire is automatically placed between the two electrical contacts.

- The switch is closed, and the capacitor discharges. The current pulse is conducted through the wire located in a gas (inert or active), producing heating through Joule effect and causing the wire to explode.

- The plasma expands in the medium due to the enormous difference in temperature and pressure between the plasma and the surrounding gas. The plasma is cooled during collisions with the surrounding gas molecules, leading to rapid condensation of the vapor into an aerosol of particles.

IV Characterization of Nanomaterials

Characterization of nanomaterials is fundamental to understanding their unique properties and optimizing their performance for various applications. Unlike bulk materials, nanomaterials exhibit size-dependent behavior influenced by their reduced dimensions, high surface-to-volume ratio, and quantum effects. Advanced characterization techniques are required to analyze their structural, compositional, optical, and mechanical properties at the nanoscale.

This chapter explores the principal methods used in nanomaterial characterization while incorporating relevant mathematical laws to provide a deeper understanding of the underlying principles.

IV .1. Structural Characterization

Structural characterization focuses on determining the size, shape, morphology, and crystal structure of nanomaterials.

IV .1.1 Transmission Electron Microscopy (TEM):

Uses high-energy electrons transmitted through a thin sample to produce high-resolution images. The resolving power of TEM is governed by the following relation:

$$\delta = \frac{0.61\lambda}{\mu \sin\theta}$$

where:

- δ is the resolution,
- λ is the wavelength of the electron beam,
- μ is the refractive index of the imaging medium,
- θ is the semi-angle of collection.

TEM provides atomic-scale resolution, allowing for detailed observation of lattice fringes, particle size, and internal defects. However, sample preparation requires precision to ensure thin, electron-transparent materials.

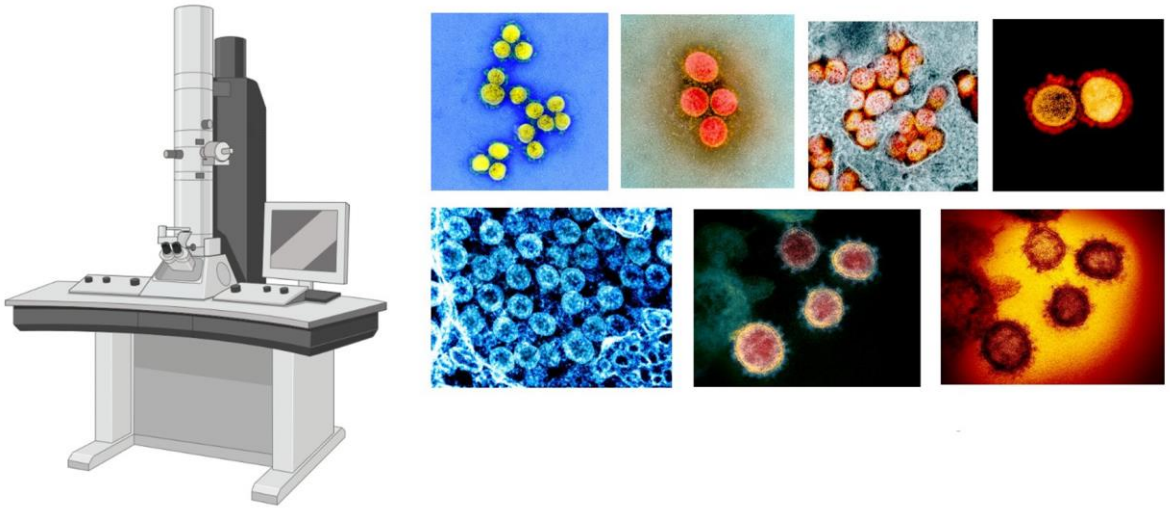

Figure 26: Transmission Electron Microscopy (TEM)

IV .1.2 Scanning Electron Microscopy (SEM):

produces surface morphology images by detecting secondary electrons emitted when a focused electron beam scans the sample. The resolution of SEM is typically lower than TEM, governed by the size of the interaction volume of the electron beam with the sample.

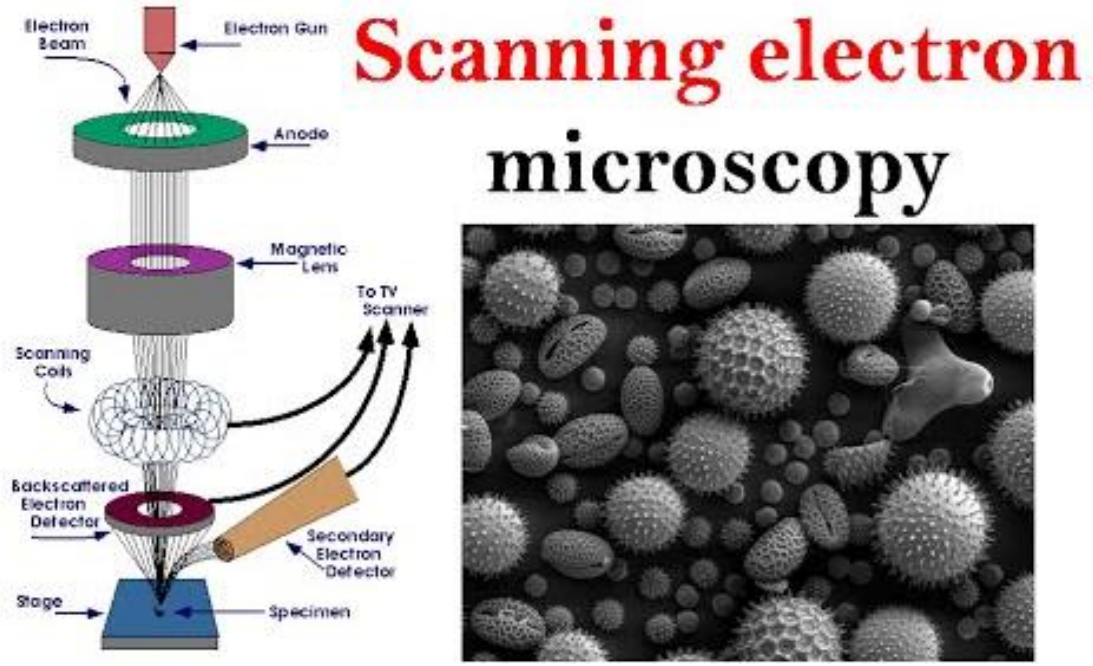

Figure 27: Scanning Electron Microscopy (SEM):

IV .1.3 Atomic Force Microscopy (AFM) :

Measures surface topography using a sharp tip that interacts with the sample. The force between the tip and the sample is described by the Lennard-Jones potential:

$$V(r) = 4\epsilon\left[\left(\frac{\sigma}{r}\right)^{12} - \left(\frac{\sigma}{r}\right)^{6}\right]$$

where:

- $V(r)$ is the potential energy,
- ϵ is the depth of the potential well,
- σ is the finite distance at which the inter-particle potential is zero,
- r is the distance between the tip and the sample surface.

AFM enables three-dimensional imaging of surfaces in various environments, providing insights into surface roughness and nanomechanical properties.

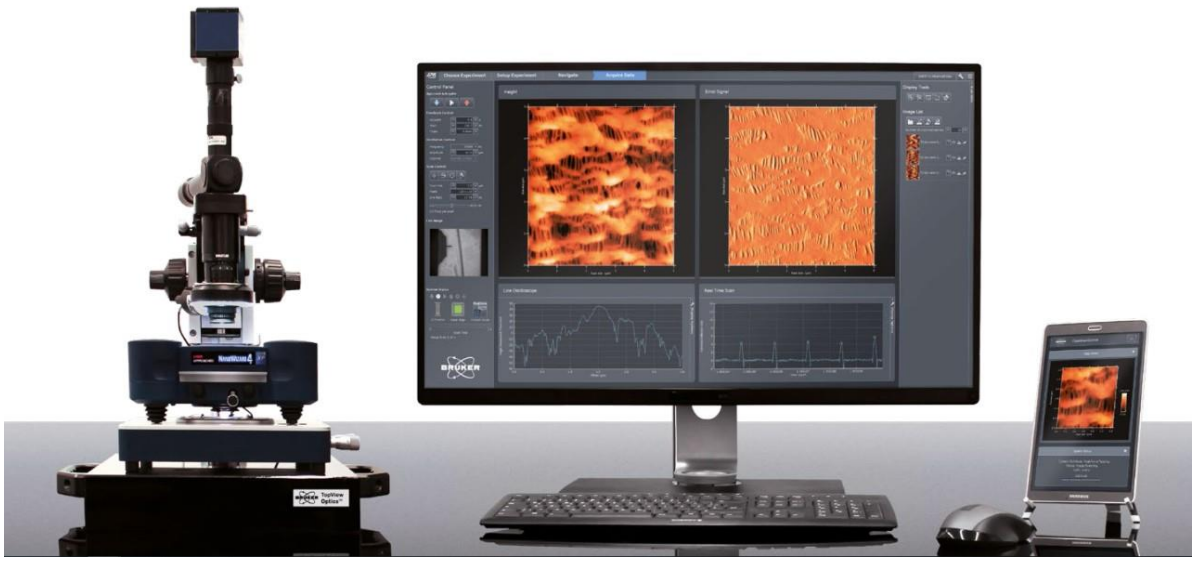

Figure 28: Atomic Force Microscopy (AFM)

IV .1.4: X-Ray Diffraction (XRD)

Determines crystal structures and grain sizes. The diffraction pattern is described by Bragg's Law:

$$n\lambda = 2d\sin\theta$$

where:

- n is the order of diffraction,
- λ is the wavelength of the incident X-rays,
- d is the interplanar spacing,
- θ is the diffraction angle.

The crystallite size (D) can be estimated using Scherrer's equation:

$$D = \frac{K\lambda}{\beta\cos\theta}$$

Where:

- K is the shape factor,
- β is the full width at half maximum (FWHM) of the diffraction peak.

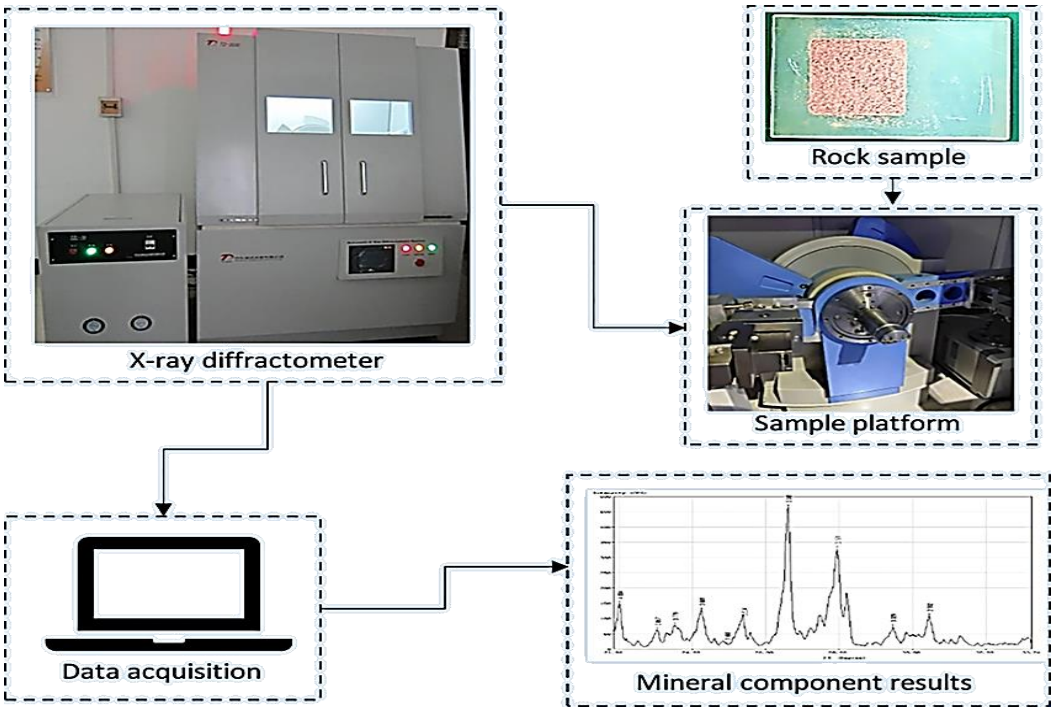

Figure 29: X-Ray Diffraction (XRD)

IV .2. Compositional Characterization

Compositional analysis identifies the elemental and chemical makeup of nanomaterials.

IV .2.1 Energy-Dispersive X-Ray Spectroscopy (EDS)

Measures characteristic X-rays emitted from the material when bombarded with high-energy electrons. The energy of these X-rays corresponds to the binding energy of electrons in specific atomic shells, providing elemental composition.

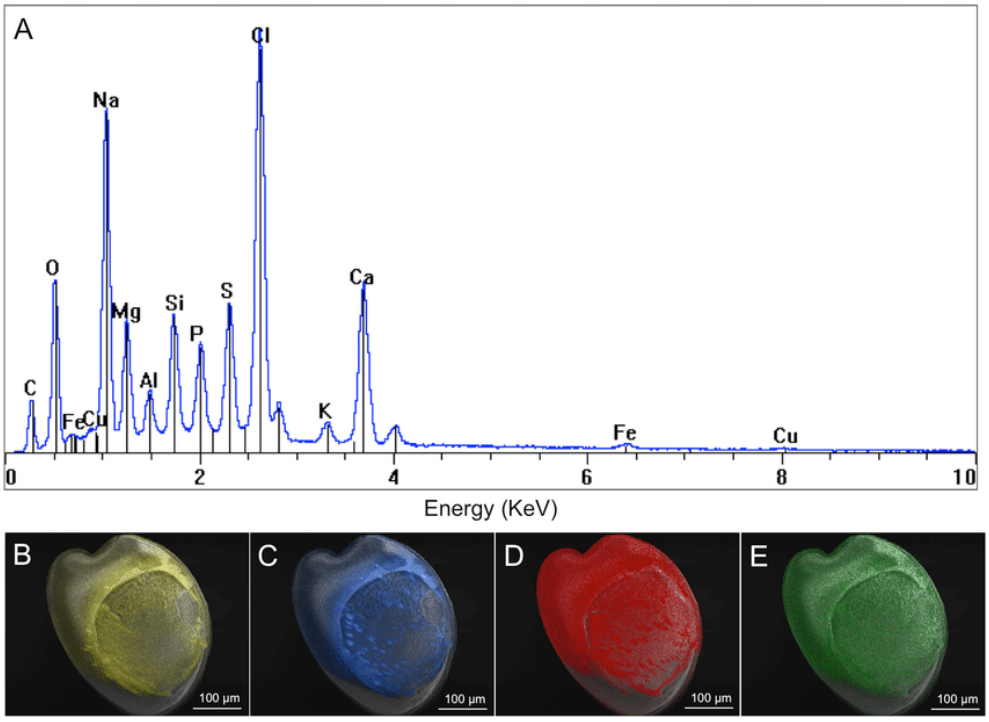

Figure 30: Energy-Dispersive X-Ray Spectroscopy (EDS)

IV .2.2 X-Ray Photoelectron Spectroscopy (XPS)

Evaluates the surface chemical composition by measuring the kinetic energy of electrons emitted under X-ray illumination. The binding energy (E_b) is given by:

$$E_b = h\nu - E_k - \phi$$

Where:

- $h\nu$ is the energy of the incident X-rays,
- E_k is the kinetic energy of the emitted electrons,

- ϕ is the work function of the detector.

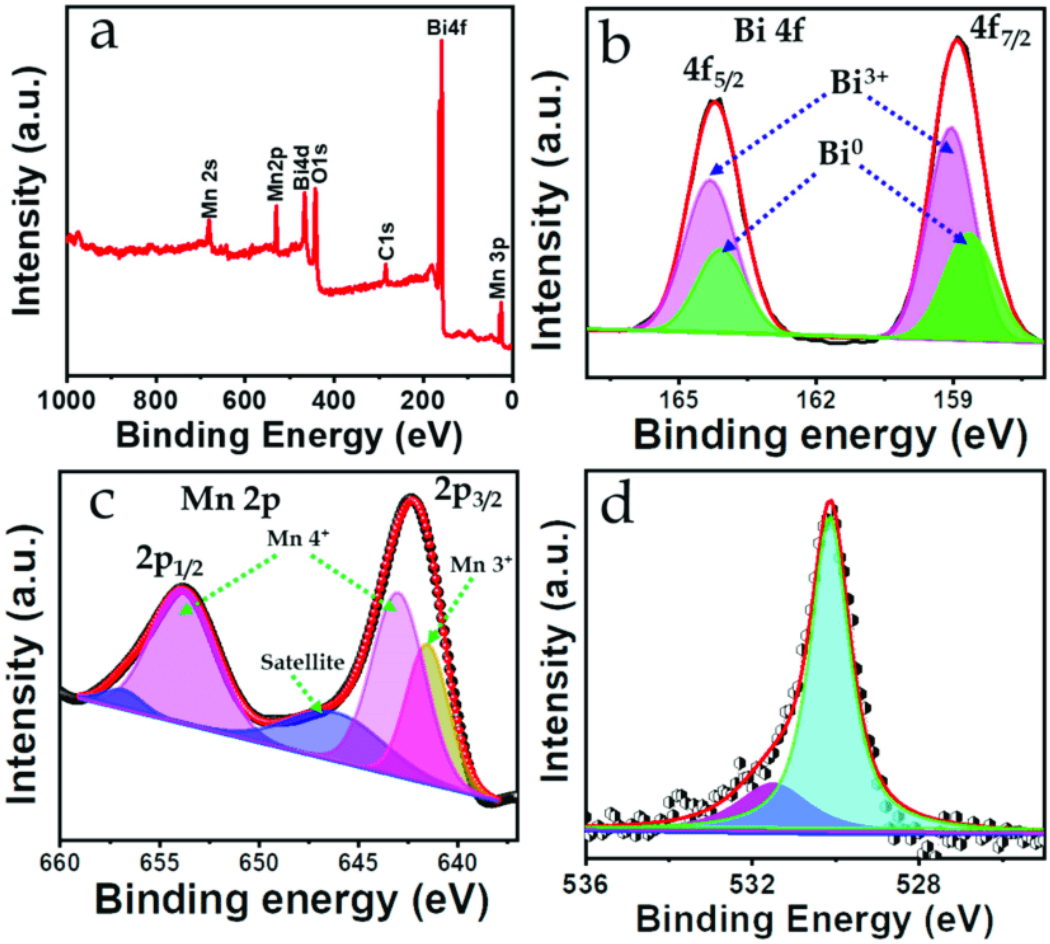

Figure 31: Ray Photoelectron Spectroscopy (XPS)

IV .2.3 Fourier Transform Infrared Spectroscopy (FTIR) :

Measures the absorption of infrared light by molecular vibrations. The absorption intensity at a specific wavelength is related to the concentration of a molecule by Beer-Lambert Law:

$$A = \epsilon c l$$

Where:

- A is the absorbance,
- ϵ is the molar absorption coefficient,

- c is the concentration,
- l is the path length of the light through the sample.

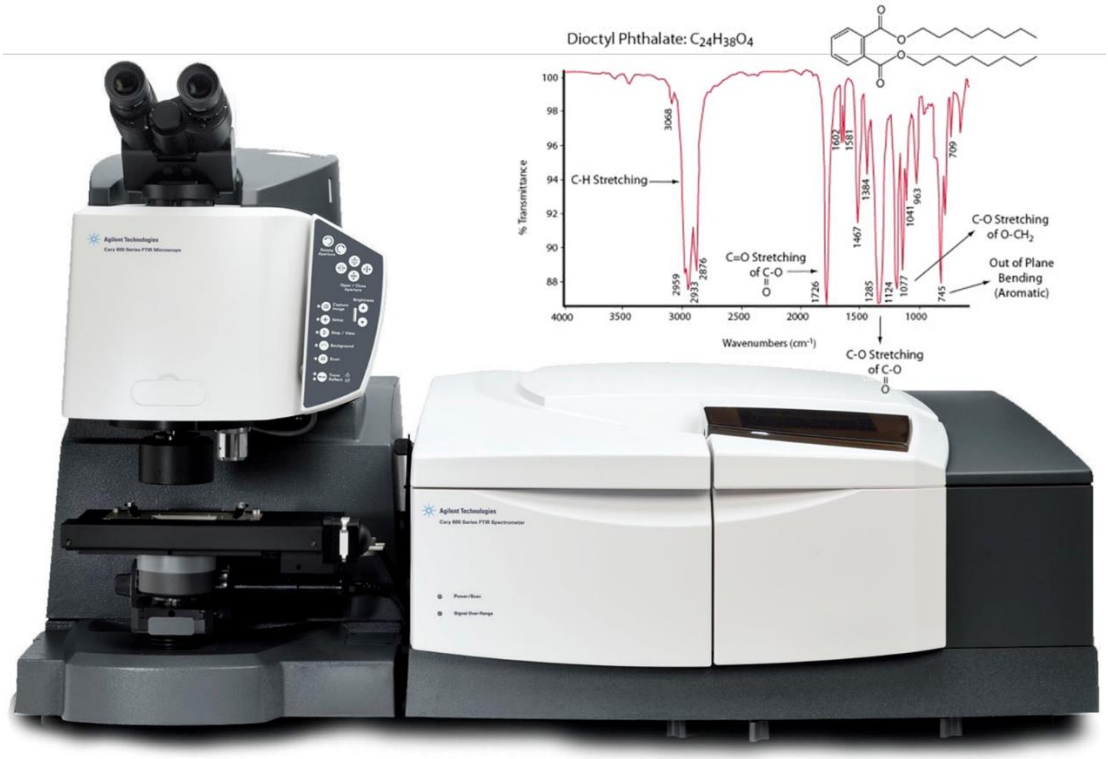

Figure 32: Fourier Transform Infrared Spectroscopy (FTIR)

IV .3. Optical Characterization

Optical characterization methods study how nanomaterials interact with light, revealing their optical and electronic properties.

IV .3.1 Ultraviolet-Visible Spectroscopy (UV-Vis)

Determines the optical bandgap of nanomaterials. The Tauc plot method is often used for semiconductors:

$$(\alpha h\nu)^n = A(h\nu - E_g)$$

Where:

- α is the absorption coefficient,

- $h\nu$ is the photon energy,
- A is a proportionality constant,
- E_g is the optical bandgap,
- n depends on the type of electronic transition (2 for direct and 1/2 for indirect transitions).

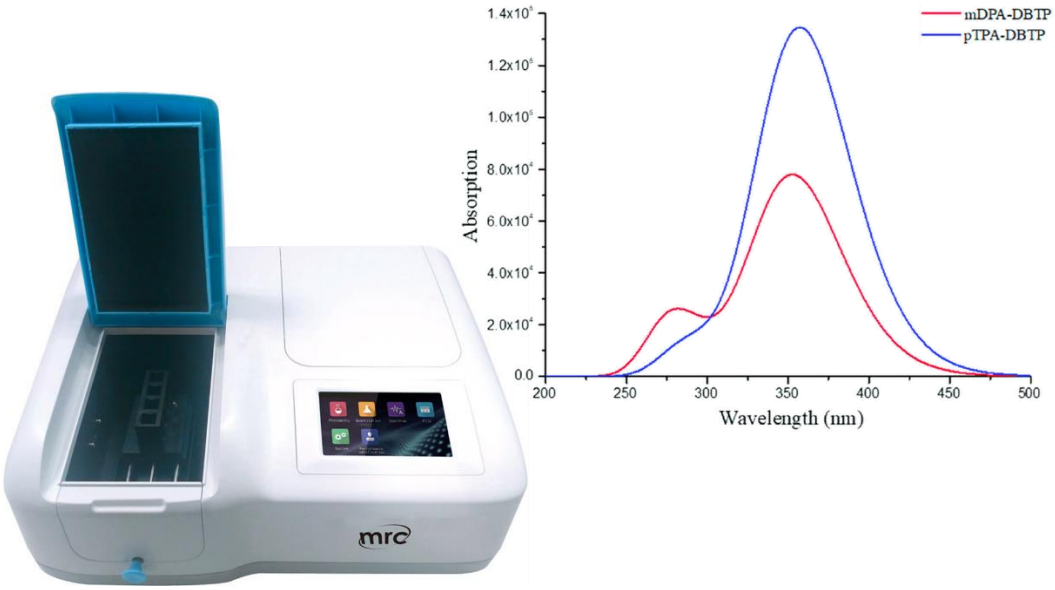

Figure 33 : Ultraviolet-Visible Spectroscopy (UV-Vis)

IV .3.2 Photoluminescence (PL) Spectroscopy

Measures the emission of light from a material after photon excitation. The intensity of PL is governed by the recombination rate of charge carriers, which is influenced by defect states and quantum confinement.

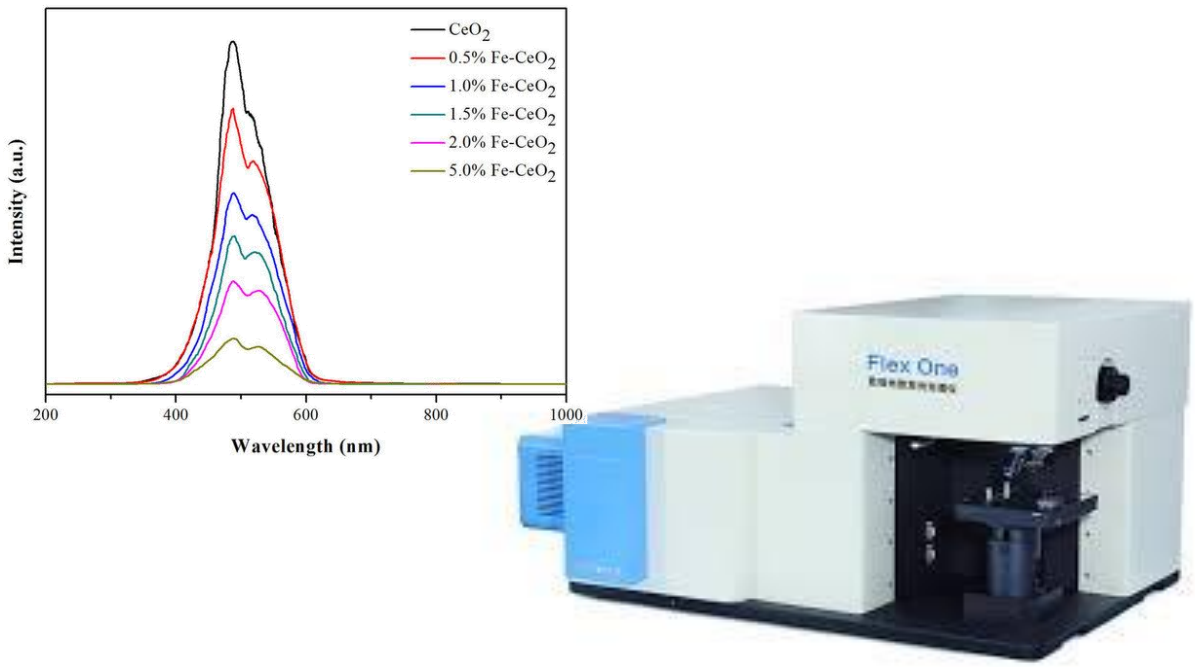

Figure 34: Photoluminescence (PL) Spectroscopy

IV .4 Mechanical Characterization

Mechanical properties of nanomaterials, such as hardness, elasticity, and toughness, are evaluated using techniques like nanoindentation and dynamic mechanical analysis.

IV .4.1 Nanoindentation

Measures hardness and elastic modulus by pressing a sharp indenter into the material and recording the force-displacement curve. The hardness (H) is given by:

$$H = \frac{F}{A}$$

Where:

- F is the applied force,
- A is the projected area of the indentation.

The elastic modulus (E) can be derived using the Oliver-Pharr method:

$$E_r = \frac{\sqrt{\pi}}{2\beta}\frac{S}{\sqrt{A}}$$

where:

- E_r is the reduced modulus,
- S is the stiffness,
- β is a geometric constant.

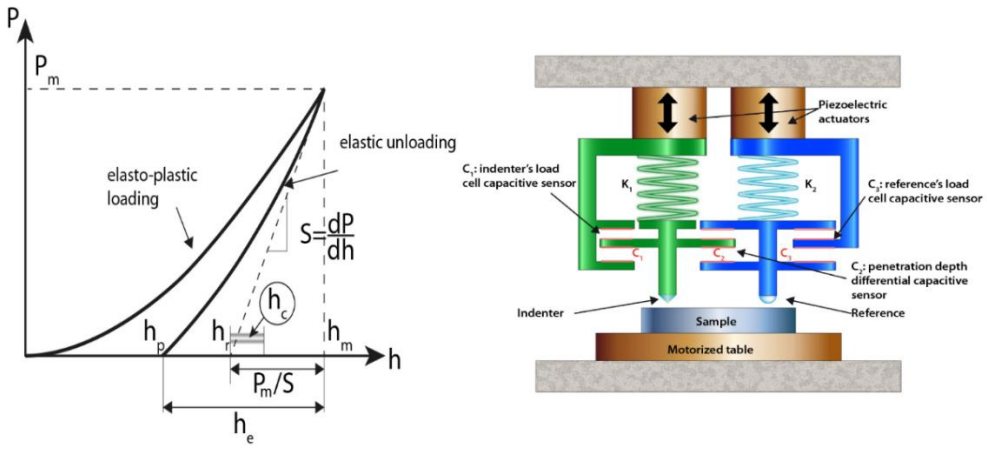

Figure 35: Nanoindentation

IV .4.2 Dynamic Mechanical Analysis (DMA)

Applies oscillatory stress to measure viscoelastic properties. The storage modulus (E') and loss modulus (E'') are calculated from the stress-strain relationship.

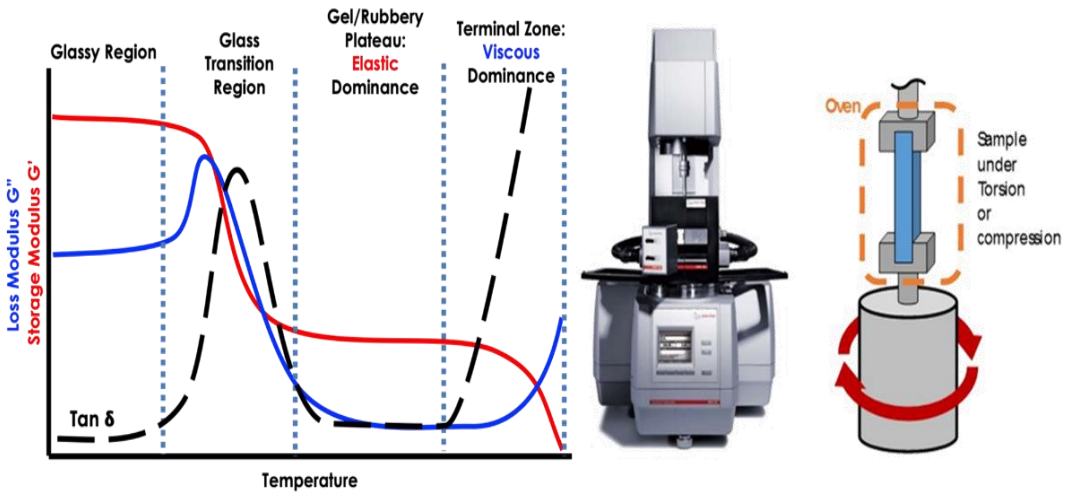

Figure 36: Dynamic Mechanical Analysis (DMA)

V. Application Domains of Nanomaterials:

Nanostructured alloys, easy to handle, are highly sought after for their mechanical, electrical, magnetic, etc., properties, which allow use in various applications. This section contains some application domains and some well-known examples in the field of shape memory alloys. It should be noted that this does not constitute an exhaustive review of all applications

V.1 Aerospace Sector:

The aerospace industry needs to minimize the volume and weight of all their components to reduce launch costs. Since Shape Memory Alloys (SMAs) offer an excellent force/density ratio and energy/weight ratio, they are excellent tools.

The Glenn Research Center at NASA has developed a new kind of tire: Superelastic. Primarily intended for future missions to Mars, it can also be a good alternative for terrestrial vehicles. Invented by the team at NASA's Glenn Research Center and Goodyear, a new airless tire is intended for future missions to Mars. But not only: NASA claims that it could also be a viable alternative to pneumatic tires on Earth.

The tire offers equal or superior traction to conventional tires and eliminates all puncture failure, thus improving automotive safety. It does not require an inner frame, simplifying and lightening the tire-wheel assembly.

The "Superelastic Tire," inspired by the Apollo lunar tires, uses shape memory alloys (mainly Nickel-Titanium (NiTi) and its derivatives) as load-bearing components. These are capable of undergoing significant reversible deformation (up to 10%) allowing the tire to withstand an order of magnitude greater deformation than other airless tires before undergoing permanent deformation.

For comparison, the rubber commonly used in tires can only be subjected to strains of about 0.3 to 0.5% before yielding, NASA specifies.

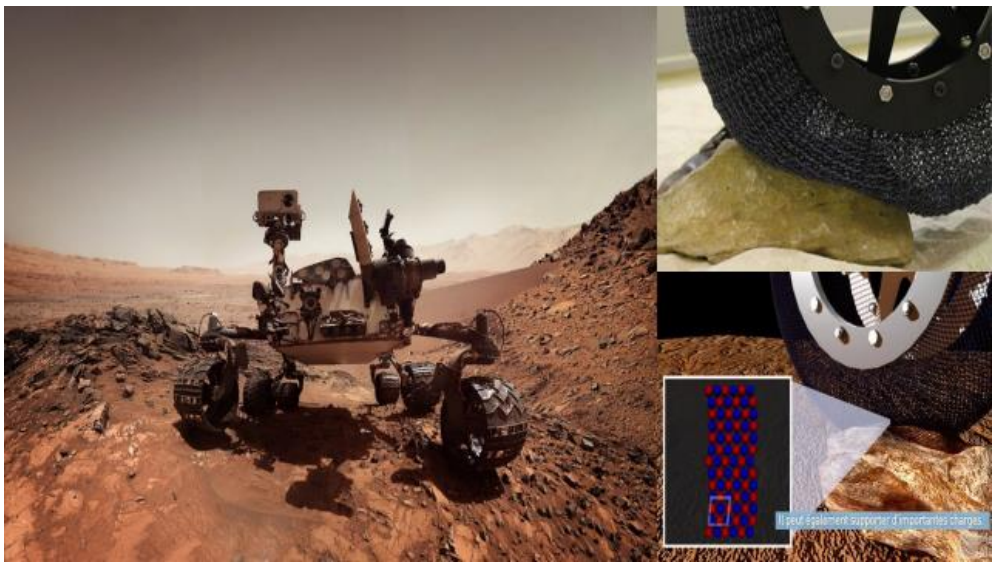

Figure 37: "Superelastic Tire," inspired by Apollo Lunar Tyres

V.2 Biomedical Sector:

This sector has very high requirements for the materials used. Moreover, this sector is probably the most active these days and particularly utilizes the superelastic effect with nitinol alloys, which are obviously biocompatible. For example, stents are devices that allow for minimally invasive surgery to counter heart problems related to partial artery obstruction.

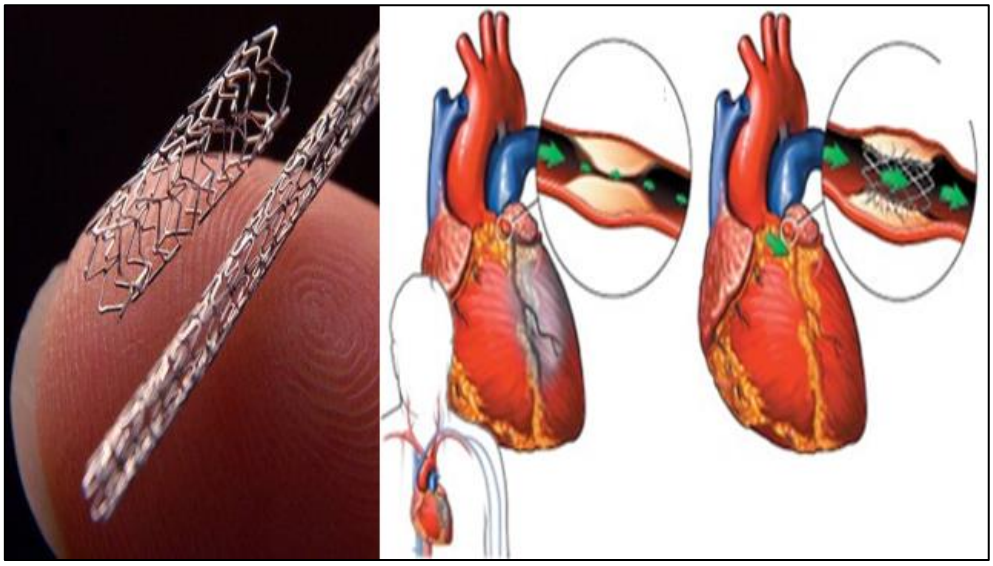

Figure 38: Stent in the Coronary Artery

Indeed, this device, once contracted, is inserted into the artery. Subsequently, upon release, the superelastic effect forces the artery to return to its original diameter, thus allowing blood flow. Similar to the stent, the heart valve shown in Figure I.20 enables minimally invasive surgery, reducing negative impacts on the patient. Finally, the last example from the biomedical sector is medical robots (nano-robots) (Figure 39). Indeed, since SMAs have a plateau in hysteresis, and their mechanical properties and biocompatibility.

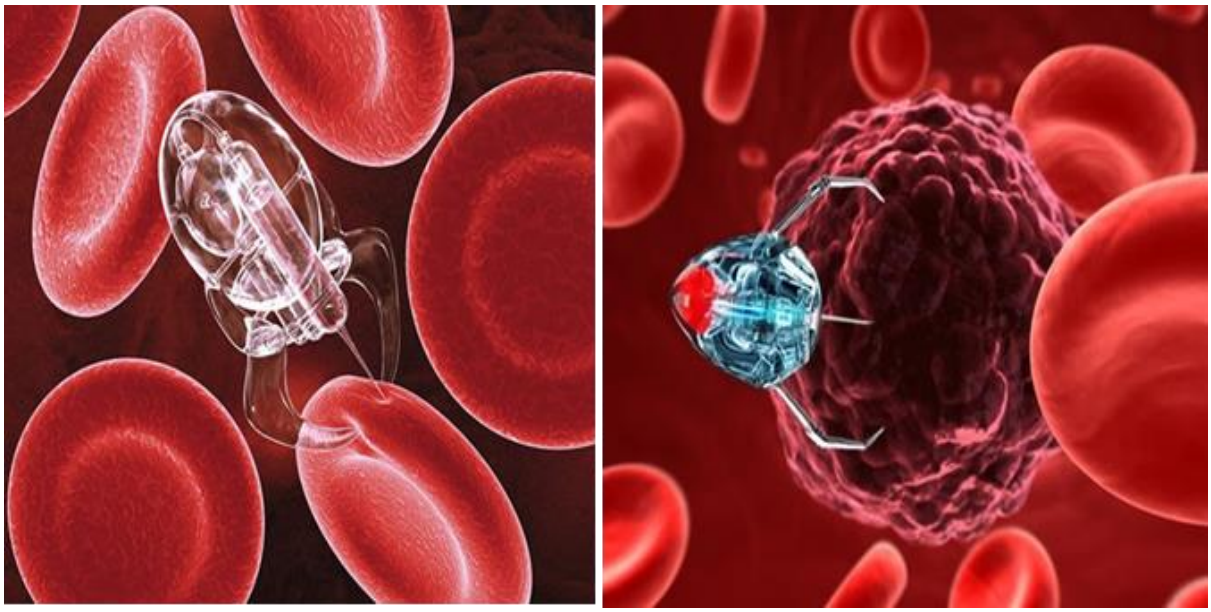

Figure 39: Medical Nanorobots

V.3 Industrial Sector:

More Functional and Intelligent Clothing:

In the 21st century, clothing is more than ever an interface between the body and the external environment, which is increasingly aggressive, polluted or even toxic, too hot, too cold, or too humid, invaded by bacteria and viruses. Future clothing will need to take this into account. Fashion designers have been thinking about this since the 1960s with the futuristic collections of André Courrèges, for example (1967).

Today, it's a new fabric that has made it possible to manufacture a shape memory shirt whose fabric lifts when it gets hot. The fabric is based on Nitinol, a shape memory alloy (SMA) containing nickel and titanium. Oricalco was developed in 2001 by the Italian Space Agency, Grado Zero Espace, as part of a technology transfer program initiated by ESA.

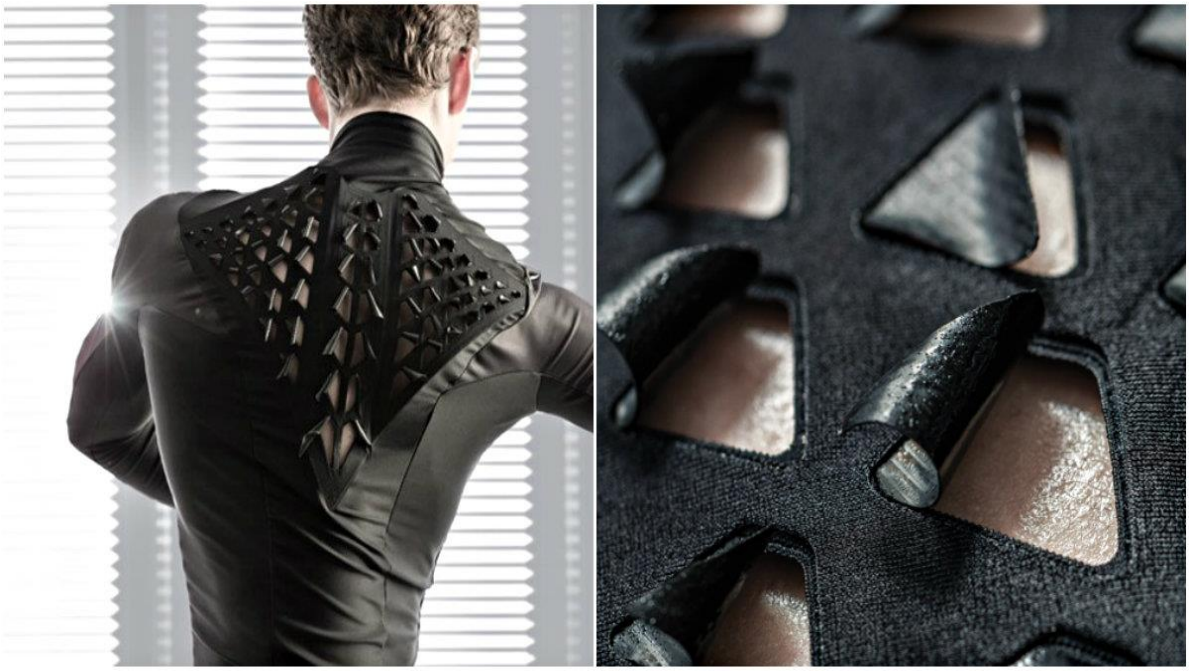

Figure 40: More Functional and Intelligent Clothing

V.4 Military Sector:

Operational drone dedicated to urban environment surveillance used by the police in the USA. Today, there are hundreds of models; France has a type of urban police drone: ELSA (Light Aircraft for Aerial Surveillance).

This represents one of the major objectives of military and police headquarters: extreme miniaturization that allows a camouflaged device to move in an urban environment as discreetly as possible, also making it less vulnerable to enemy fire.

The second mission assigned to these future insects is indoor flight for observation, surveillance, reconnaissance, espionage missions, or even attacks [kamikaze insect robot that can explode]. A new weapon against simple protesters,

political opponents, urban guerrillas, who could take advantage of the large city to hide, conceal, protect themselves.

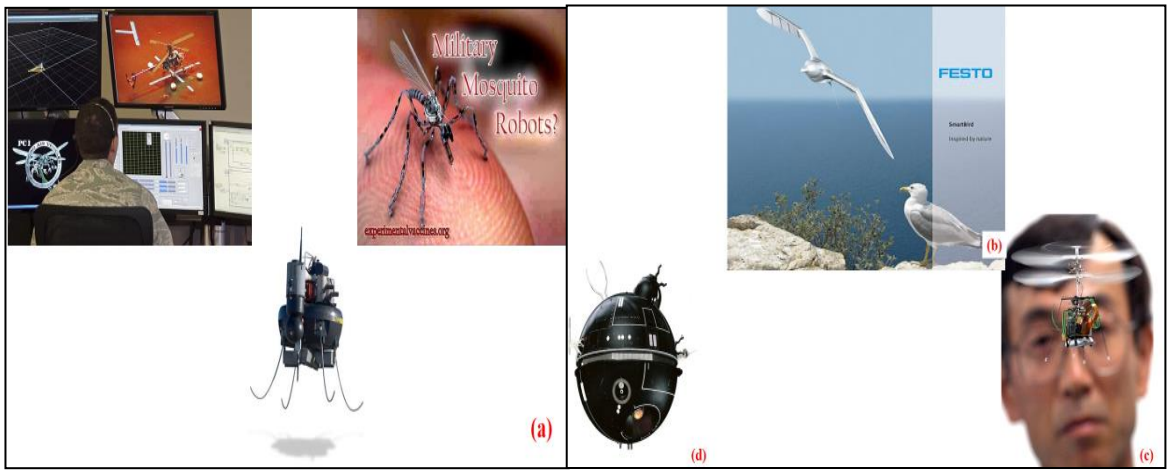

Figure 41: (a) Drone / United States; (b) Drone / Germany [SmartBird]; (c) Drone / China; (d) Drone / Japan

References:

[1] Bououdina, Mohamed (ed.). *Handbook of research on nanoscience, nanotechnology, and advanced materials*. IGI Global, 2014.

[2] Shunin, Y., Bellucci, S., Gruodis, A., Lobanova-Shunina, T.: Nanotechnology Application Challenges: Nanomanagement, Nanorisks and Consumer Behaviour Nonregular Nanosystems 337-395 (2018).

[3] Shunin, Yuri, Bellucci, Stefano, Gruodis, Alytis, *et al. Nonregular Nanosystems*. Springer, 2018.

[4] Suryanarayana, C. Nanoparticle synthesis. *Materials today*, 2005, vol. 8, no 11, p. 62.

[5] Suryanarayana, C. Et Al-aqeeli, Nasser. Mechanically alloyed nanocomposites. *Progress in Materials Science*, 2013, vol. 58, no 4, p. 383-502.

[6] Suryanarayana, C.: Mat. Sci and Eng A 479, 23(2008).

[7] Parizeau, Marie-Hélène. L'éthique des nanotechnologies: vers un élargissement de l'évaluation des risques? *À chacun son développement durable? De la diversité culturelle aux nanotechnologies*, 2017, p. 299.

[8] Busk, S.A.: Nanostructured titanium dioxide: Fate in the aquatic environment and effects on the blue mussel Mytilus edulis, Department of Mathematics and Natural Sciences Spring (2011).

[9] Farvizi, M.: Arch. Metall. Mater. 62, 2B, 1075-1079 (2017).

[10] http://www.astrosurf.com/luxorion/technologiesfutur3.htm#:~:text=L'Oricalco%20a%20%C3%A9t%C3%A9%20d%C3%A9velopp%C3%A9,technologies%20initi%C3%A9%20par%20l'ESA.

[11] https://en.wikipedia.org/wiki/Nanotechnology

[12] https://ec.europa.eu/health/scientific_committees/opinions_layman/en/nanotechnologies/index.htm#1

[13] https://technology.nasa.gov/patent/LEW-TOPS-99